

Effect of elevated
CO₂ on organic
matter pools and
fluxes in a summer

A. J. Paul et al.

Effect of elevated CO₂ on organic matter pools and fluxes in a summer, post spring-bloom Baltic Sea plankton community

A. J. Paul¹, L. T. Bach¹, K.-G. Schulz^{1,2}, T. Boxhammer¹, J. Czerny¹,
E. P. Achterberg^{1,3}, D. Hellemann^{1,4}, Y. Trense^{1,*}, M. Nausch⁵, M. Sswat¹, and
U. Riebesell¹

¹GEOMAR Helmholtz Centre for Ocean Research Kiel, Düsternbrooker Weg 20, 24105 Kiel, Germany

²Southern Cross University, Military Road, East Lismore, NSW 2480, Australia

³National Oceanography Centre Southampton, European Way, University of Southampton, Southampton SO14 3ZH, UK

⁴Department of Environmental Sciences, University of Helsinki, PL 65 00014 Helsinki, Finland

⁵Leibniz Institute for Baltic Sea Research, Seestrasse 15, 18119 Rostock, Germany

* now at: Comprehensive Centre for Inflammation Medicine, University of Lübeck, Ratzeburger Allee 160, 23538 Lübeck, Germany

Title Page

Abstract

Introduction

Conclusions

References

Tables

Figures

⏪

⏩

◀

▶

Back

Close

Full Screen / Esc

Printer-friendly Version

Interactive Discussion



Received: 1 April 2015 – Accepted: 10 April 2015 – Published: 6 May 2015

Correspondence to: A. J. Paul (apaul@geomar.de)

Published by Copernicus Publications on behalf of the European Geosciences Union.

BGD

12, 6863–6927, 2015

**Effect of elevated
CO₂ on organic
matter pools and
fluxes in a summer**

A. J. Paul et al.

Title Page

Abstract

Introduction

Conclusions

References

Tables

Figures



Back

Close

Full Screen / Esc

Printer-friendly Version

Interactive Discussion



Abstract

Ocean acidification is expected to influence plankton community structure and biogeochemical element cycles. To date, experiments with nutrient stimulated blooms have been primarily used to study the response of plankton communities to elevated CO₂.

In this CO₂ manipulation study, we used large-volume (~ 55 m³) pelagic in situ mesocosms to enclose a natural, post spring-bloom plankton assemblage in the Baltic Sea to investigate the response of organic matter pools to ocean acidification. In the mesocosms, *f*CO₂ was manipulated yielding a range of average *f*CO₂ of 365 to ~ 1231 µatm with no adjustment of naturally available nutrient concentrations. Plankton community development and key biogeochemical element pools were subsequently followed in this nitrogen-limited ecosystem over a period of seven weeks.

We identified three distinct phases based on temperature fluctuations and plankton biomass: a warm, productive period with elevated chlorophyll *a* and particulate matter concentrations (Phase I), a decline in autotrophic biomass coinciding with cooler water temperatures associated with lower incoming photosynthetically active radiation (PAR) and higher zooplankton grazing pressure (Phase II), and a steady state phase with low net change in particulate and dissolved matter pools (Phase III). We observed higher sustained chlorophyll *a* and particulate matter concentrations (~ 25 % higher) and lower inorganic phosphate concentrations in the water column in the highest *f*CO₂ treatment (1231 µatm) in Phase III. Size-fractionated phytoplankton pigment analyses indicated that these differences were driven by picophytoplankton (< 2 µm) and were already established early in the experiment during Phase I. However the influence of picophytoplankton on bulk organic matter pools was masked by high biomass of larger plankton until Phase III when the small size fraction (< 2 µm) contributed up to 90 % of chlorophyll *a*. Furthermore, CO₂-related differences in water column suspended matter concentrations were not reflected in sinking material flux. Our results from this study indicate that ocean acidification could have significant and sustained impacts on pelagic biogeochemical element pools in nitrogen-limited ecosystems.

BGD

12, 6863–6927, 2015

Effect of elevated CO₂ on organic matter pools and fluxes in a summer

A. J. Paul et al.

Title Page

Abstract

Introduction

Conclusions

References

Tables

Figures

◀

▶

◀

▶

Back

Close

Full Screen / Esc

Printer-friendly Version

Interactive Discussion



1 Introduction

The Baltic Sea is a semi-enclosed, brackish, epicontinental sea with a substantial fresh-water catchment area which is approximately four times larger than the water body itself. In addition, the Baltic Sea has limited and infrequent saline deep water inputs from the North Sea through the Danish straits which form an important oxygen supply for the Baltic Sea bottom waters. Weak circulation, vertical mixing and water mass exchange in the Baltic Sea leads to strong horizontal and vertical salinity gradients (surface waters from north (< 5) to south (~ 20) Baltic, and surface (~ 7) to deep (~ 12) at station BY15 at Gotland Deep, The International Council for the Exploration of the Sea, 2014). Consequently, the enclosed nature of the water body and minimal water exchange mean that terrestrial and anthropogenic activities have a considerable influence on water quality, biogeochemistry and ecosystems in the Baltic Sea.

Global change is expected to have pronounced effects on the physical and chemical conditions in the Baltic Sea. Warming, decreasing pH, and increasing freshwater inputs are expected to affect primary productivity and decrease oxygen concentrations in the deeper basins (HELCOM, 2013). In combination with higher nutrient loads from changes in agricultural activity this may lead to increased hypoxia or even anoxia in sub-surface waters (Meier et al., 2011) with feedbacks on biogeochemical element cycles (Sutton et al., 2011), and ecosystem structure and functioning particularly at higher trophic levels (Ekau et al., 2010; Turner, 2001; Wu, 2002). Changes in the Baltic Sea environment have already been detected. Regular monitoring of the Baltic Sea over the past 100 years has indicated higher rates of temperature increase (0.08 to 0.11 °C per decade) than the global average, along with a 20 % decrease in annual maximum ice extent (HELCOM, 2013). Observed shifts in the spring and summer phytoplankton community dynamics have been primarily associated with warming in northern Baltic Sea regions over the past three decades (Suikkanen et al., 2013).

Ocean acidification is another anthropogenic process of potential relevance for Baltic plankton communities. As CO₂ dissolves in seawater, the carbonate system shifts with

BGD

12, 6863–6927, 2015

Effect of elevated CO₂ on organic matter pools and fluxes in a summer

A. J. Paul et al.

Title Page

Abstract

Introduction

Conclusions

References

Tables

Figures



Back

Close

Full Screen / Esc

Printer-friendly Version

Interactive Discussion



an associated decrease in pH. Ocean acidification therefore adds to the decrease in seawater pH as a result of nitrogen and sulphate deposition in the form of acid rain (Doney et al., 2007). Between 1993 and 2012, pH in the Baltic Proper decreased on the order of 0.1 pH units (The International Council for the Exploration of the Sea, 2014) which is more than two times faster than observed in the Pacific Ocean (Fig. 1, ~ 0.04 pH decrease between 1992 and 2012 in surface 30 m, Station ALOHA, Hawaii Ocean Time-Series, Dore et al., 2009). Changes in $f\text{CO}_2$ and pH influence phytoplankton physiology, growth rates, and carbon fixation with some phytoplankton functional groups, such as calcifying organisms, more sensitive than others such as diatoms (Riebesell and Tortell, 2011; Rost et al., 2008). Thus the relative fitness of each functional group determines the response of the plankton community as a whole. Changes in physiological processes in phytoplankton on a cellular level can cascade through trophic levels and induce shifts in structure of the planktonic food web.

To date, the majority of ocean acidification experiments have utilised nutrient replete starting conditions or added nutrients to investigate effects of high CO_2 on plankton communities and biogeochemical cycles (Table 1). These studies mimic the productive spring bloom where nutrient concentrations are relatively high and light initially limits phytoplankton growth. However for considerable parts of the year, the opposite is the case. Growth is not limited by light but by nutrient concentrations and biomass tends to be low. This is also the case during summer in the Baltic Sea. Here, a diatom-dominated spring bloom in April/May usually draws down dissolved inorganic nutrients so that concentrations remain low from early summer. Diazotrophic filamentous cyanobacteria then commonly bloom in July and August when surface water temperatures peak, calm weather conditions induce water column stratification and low nitrogen in a bioavailable form limits growth in the non-diazotrophic phytoplankton (Gasiūnaitė et al., 2005; Kanoshina et al., 2003; Stal et al., 1999).

We undertook a pelagic in situ mesocosm study on a summer Baltic Sea plankton community to investigate the response of this low nutrient ecosystem to projected changes in $f\text{CO}_2$. Many different trophic levels from bacteria and viruses through to

BGD

12, 6863–6927, 2015

Effect of elevated CO_2 on organic matter pools and fluxes in a summer

A. J. Paul et al.

Title Page

Abstract

Introduction

Conclusions

References

Tables

Figures

◀

▶

◀

▶

Back

Close

Full Screen / Esc

Printer-friendly Version

Interactive Discussion



5 timeline including important manipulations. Mesocosm bags were cleaned occasionally inside and outside throughout the experiment to minimise wall growth and keep the biofilm biomass at a minimum (see Fig. 4 and Riebesell et al. (2013) for further details). At the end of the experiment, the volume of each mesocosm (0–19 m) was determined through addition of a calibrated salt solution as described by Czerny et al. (2013). Final mesocosm volumes ranged between 53.1 and 55.1 m³ with an estimated uncertainty of 2%. Unfortunately three mesocosms (M2, M4 and M9) were lost because of extensive and unquantifiable water exchange with the surrounding seawater due to a welding error on the mesocosm bags, and were thus excluded from sampling and analyses.

10 2.2 CO₂ manipulations

CO₂ treatments were achieved by equally distributing filtered (50 µm), CO₂-saturated seawater into the mesocosm as described by Riebesell et al. (2013) in four separate additions (see Table 2 for details). The first addition of CO₂-enriched seawater defined the beginning of the experiment and took place on *t*₀ following sampling activities. 15 Seawater for the additions was collected from 10 m depth by a pipe connected to the laboratory in the research station. Different amounts of CO₂-saturated seawater were added to four mesocosms to set-up an initial gradient in *f*CO₂ treatments from ambient (~ 240 µatm) up to ~ 1650 µatm. On *t*₁₅, CO₂ was manipulated in the upper 7 m to counteract pronounced outgassing in the mesocosm. Two mesocosms were selected 20 as controls with no addition of CO₂-enriched seawater. Instead unenriched filtered seawater (50 µm) was added for the initial manipulations. For the later smaller addition, the water distributor (“spider”, Riebesell et al., 2013) was pulled up and down in each mesocosm to simulate water column mixing and manipulation side effects caused by the device on *t*₁₅.

BGD

12, 6863–6927, 2015

Effect of elevated CO₂ on organic matter pools and fluxes in a summer

A. J. Paul et al.

Title Page

Abstract

Introduction

Conclusions

References

Tables

Figures

⏪

⏩

◀

▶

Back

Close

Full Screen / Esc

Printer-friendly Version

Interactive Discussion



2.3 CTD and light measurements

CTD casts in each mesocosm and in the surrounding water were made with a hand-held self-logging CTD60M probe (Sea and Sun Technology) from 0.3 down to ~ 18 m (mesocosms) and to ~ 30 m (surrounding water) between 13:30 and 14:30 LT daily until *t*31, and then every second day until *t*46. Temperature, pH, dissolved oxygen and PAR (photosynthetic active radiation) sensors were deployed on the CTD as well as a conductivity cell. Details on the sensors, their accuracy and precision and corrections applied are described in Schulz and Riebesell (2013). The potentiometric CTD pH was corrected to spectrophotometric measurements (see Sect. 2.5.1). The depth of average water column light intensity in metres was calculated by averaging all water column PAR (photosynthetically active radiation) data and relating this to the depth where this intensity of PAR occurred.

A LICOR LI192 PAR sensor was placed unobstructed at the end of a 2 m pole on the roof of Tvärminne Zoological Station (~ 1 km from mesocosm mooring site) to record incoming PAR for the mesocosms. Incoming PAR was recorded from 14:43 LT, on 14 June 2012 continuously as the mean of integrated 60 s intervals until the end of the experiment at 11:23 LT on 7 August 2012.

2.4 Sampling procedures

Water samples were collected regularly from each mesocosm and the surrounding water using depth-integrated water samplers (IWS, HYDRO-BIOS Kiel). Unless otherwise reported, all samples are from the entire water column (0 to 17 m). For example, inorganic dissolved nutrient and fluorometric Chl *a* samples were also taken regularly for the upper water column (0 to 10 m). Full details of mesocosm sampling procedures and equipment are described in Riebesell et al. (2013) and Schulz et al. (2013). There were two intensive sampling periods where sampling took place every day (*t*3 to *t*5, *t*29 to *t*31), otherwise most parameters were sampled every second day. Chl *a* was sampled daily for analysis by fluorometry until *t*31 and carbonate chemistry until *t*17 after

BGD

12, 6863–6927, 2015

Effect of elevated CO₂ on organic matter pools and fluxes in a summer

A. J. Paul et al.

Title Page

Abstract

Introduction

Conclusions

References

Tables

Figures



Back

Close

Full Screen / Esc

Printer-friendly Version

Interactive Discussion



Effect of elevated CO₂ on organic matter pools and fluxes in a summer

A. J. Paul et al.

Title Page

Abstract

Introduction

Conclusions

References

Tables

Figures



Back

Close

Full Screen / Esc

Printer-friendly Version

Interactive Discussion



when these parameters were also sampled every second day. Sampling for dissolved organic phosphorus (DOP) continued only until *t*30 and Chl *a* until *t*39, but for all other parameters until *t*43. Samples for carbonate chemistry variables and trace gas analyses were the first to be sampled and were taken from the IWS directly on board the sampling boat. Other samples (e.g. particulate matter, Chl *a*, phytoplankton pigments) were collected into 10 L carboys and stored in the dark. Carboys were stored at in situ temperature on-shore and sub-sampling from these carboys was usually within one hour and up to a maximum of 5 h after sampling. Care was taken to mix the water samples in the carboys well before taking subsamples to ensure homogeneous sampling for all parameters.

The sediment trap was emptied every second day using a manual vacuum pump system to acquire the settled material via a silicon tube reaching down to the collection cylinder of the sediment trap (Boxhammer et al., 2015; Riebesell et al., 2013). This material was used to quantify and characterise particle sinking flux. Subsamples of the particle suspension (< 6% in total) were taken before the material was concentrated. Particles and aggregates were allowed to settle down within 2 h at in situ temperature before separation of the supernatant. Collected particulate material was then centrifuged, while subsamples of the supernatant were filtered and analysed analogous to water column samples for particulate matter. Centrifuged material was subsequently frozen, lyophilised and ground to a fine powder of homogeneous composition. From this powder small subsamples of between 0.7 and 1.5 mg were weighed and analysed for carbon, nitrogen, phosphate and biogenic silica content as described in this manuscript for water column samples (see Sect. 2.5.3). Concentrations of particulate material were calculated based on total mesocosm volume in L. Mesocosm volume determined on *t*45 by salt addition in kg (Sect. 2.2) was converted using mean mesocosm temperature and salinity over 0–17 m between *t*3 and *t*43 (mean temperature = 11.415 °C, mean salinity = 5.698) and the algorithms described by Fofonoff and Millard Jr. (1983). A more in-depth description of sampling and processing of particu-

late material collected in the sediment traps of the KOSMOS setup will be presented in Boxhammer et al. (2015).

2.5 Sample analyses

2.5.1 Carbonate system parameters (DIC, TA, pH_T)

5 Samples for total alkalinity (TA), dissolved inorganic carbon concentrations (DIC) and total pH (pH_T) were gently pressure-filtered (Sarstedt Filtropur PES 0.2 μm) using a membrane pump (Stepdos) to exclude calcareous particles and particulate organic material before analysis. Presence of particulate matter can influence precision of carbonate chemistry measurements. In addition, the sterile filtration eliminates the influ-
10 ence of biological processes on pH and DIC during sample storage by phytoplankton or bacteria.

Total pH was determined by spectrophotometry as described in Dickson et al. (2007). Samples were analysed on a Cary 100 (Varian) spectrophotometer in a temperature controlled 10 cm cuvette using a low ionic strength m-cresol indicator dye matching the
15 salinity of the sample water and an appropriate low salinity pK (Mosley et al., 2004). For further information on analytical procedure and dye preparation and precision, see Schulz et al.,(in prep.). CTD pH measurements were corrected to pH_T by daily linear correlations of mean water column potentiometric pH measurements to spectrophotometric pH_T measurements.

20 DIC concentrations were determined by infrared absorption using a LICOR LI-7000 on an AIRICA system (MARIANDA, Kiel). Measurements were made on four replicates of 2 mL sample volume and DIC was calculated as the mean of the best three out of four measurements. The precision was typically better than 1.5 μmol kg⁻¹. Dissolved calcium concentrations in seawater were determined by inductively coupled plasma optical emission spectroscopy (ICP-OES) using a VARIAN 720-ES and IAPSO reference
25 material.

BGD

12, 6863–6927, 2015

Effect of elevated CO₂ on organic matter pools and fluxes in a summer

A. J. Paul et al.

Title Page

Abstract

Introduction

Conclusions

References

Tables

Figures

◀

▶

◀

▶

Back

Close

Full Screen / Esc

Printer-friendly Version

Interactive Discussion



Effect of elevated CO₂ on organic matter pools and fluxes in a summer

A. J. Paul et al.

Title Page

Abstract

Introduction

Conclusions

References

Tables

Figures

◀

▶

◀

▶

Back

Close

Full Screen / Esc

Printer-friendly Version

Interactive Discussion



TA was analysed by potentiometric titration using a Metrohm 869 Sample Changer and a 907 Titrand Dosing unit according to the open cell method described in Dickson et al. (2007). Due to unaccounted contributions to TA in the range of 20 and 25 $\mu\text{mol kg}^{-1}$ by components such as organic acids and bases, spectrophotometric pH_T and DIC were used to calculate carbonate chemistry speciation using the stoichiometric equilibrium constants for carbonic acid of Mehrbach et al. (1973) as refitted by Lueker et al. (2000). Buffering by organic compounds is not accounted for in the traditional TA definition (Dickson, 1981) and depends on unknown concentrations and acid/base equilibria of certain DOM components. Thus, using TA for carbonate chemistry speciation calculations would have resulted in errors (Koeve and Oschlies, 2012). Both TA and DIC measurements were calibrated against accompanying measurements of the certified reference material batch, CRM 115 (Dickson, 2010).

2.5.2 Dissolved inorganic nutrients

Samples for nutrients were collected in acid-cleaned (1 mol L^{-1} HCl) 60 mL low density polyethylene bottles (Nalgene), stored at 4°C in the dark following sampling and analysed within 12 h of collection. Dissolved silicate (DSi) concentrations were determined using standard colorimetric techniques (Grasshoff et al., 1983) at the micromolar level using a nutrient autoanalyser (Seal Analytical, Quattro). Nanomolar levels of dissolved nitrate + nitrite (hereafter nitrate) and dissolved inorganic phosphate (DIP) were determined with a colorimetric method using a 2 m liquid waveguide capillary cell (LWCCs) (Patey et al., 2008; Zhang and Chi, 2002) with a miniaturised detector (Ocean Optics Ltd). Detection limits were 2 nmol L^{-1} for nitrate and 1 nmol L^{-1} for DIP, with a linear range up to 300 nmol L^{-1} . All samples for inorganic nutrient measurements were filtered using glass fibre filters (GF/F, nominal pore size of $0.7 \mu\text{m}$, Fisher Scientific) prior to analysis. This was done to reduce the dissolution of nutrients from particulates during analysis, and also to avoid particles blocking the LWCCs and interfering with the spectrophotometric measurements. Ammonium (NH_4^+) measurements were under-

taken following the method by K erouel and Aminot (1997) with fluorimetric detection (Trilogy, Turner), and featuring a detection limit of 5 nmol L⁻¹.

2.5.3 Particulate material (C, N, P, Si)

Total particulate carbon, particulate organic nitrogen and total particulate phosphorus (TPC, PON, TPP) samples were collected onto combusted GF/F filters (Whatman, nominal pore size of 0.7  m) using gentle vacuum filtration (< 200 mbar) and stored in glass petri dishes at -20  C directly after filtration until analysis. Filters and glass petri dishes were combusted at 450  C for 6 h before use. Filters were not acidified to distinguish between inorganic and organic particulate carbon before analyses hence we measured TPC. However, microscopy counts and total alkalinity drawdown indicated pelagic calcifying organisms were not abundant and there was no significant calcification, thus it was probably mostly particulate organic carbon. In addition to the total particulate matter fraction, gauze pre-filters were used to separate size-fractionated samples for C and N analyses (0.7 to 10  m = TPC/PON_{<10}, 0.7 to 55  m = TPC/PON_{<55}). Filtration volumes ranged from 500 mL for the total fraction (POM_{tot}) to up to 1500 mL for < 55  m size fraction to ensure sufficient biomass on the filter for analyses.

Filters for TPC/PON were dried at 60  C, packed into tin capsules and stored in a dessicator until analysis. TPC and PON measurements were made on an elemental analyser (EuroEA) according to Sharp (1974), coupled by either a Conflo II to a Finnigan Delta^{Plus} isotope ratio mass spectrometer or a Conflo III to a Thermo Finnigan Delta^{Plus} XP isotope ratio mass spectrometer. Sediment material powder was weighed directly into tin capsules using a Sartorius M2P electronic microbalance with an accuracy of 0.001 mg. In addition to the standard calibration at the beginning of each run, standard materials (caffeine, peptone, acetanilide, nicotinamide, glutamic acid) were also included within runs to identify any drift and ensure accuracy and full combustion of the samples during analysis. Selected samples for sediment material TPC and PON were reanalysed on an elemental analyser (EuroEA) not coupled to a mass spectrometer using the same method and standard materials. Total sinking particle flux is the

BGD

12, 6863–6927, 2015

Effect of elevated CO₂ on organic matter pools and fluxes in a summer

A. J. Paul et al.

Title Page

Abstract

Introduction

Conclusions

References

Tables

Figures

⏪

⏩

◀

▶

Back

Close

Full Screen / Esc

Printer-friendly Version

Interactive Discussion



sum of both the particulate matter concentrations determined in sediment powder and supernatant.

Filters for total particulate phosphorus (TPP) were placed in 40 mL of deionised water (MilliQ, Millipore) water with oxidising decomposition reagent (MERCK, Catalogue no. 112936) and autoclaved for 30 min in a pressure cooker to oxidise the organic phosphorus to orthophosphate. Samples were allowed to cool before concentrations were determined by spectrophotometric analysis as for dissolved inorganic phosphate concentrations according to Hansen and Koroleff (1999).

For biogenic silica (BSi), samples were collected on cellulose acetate filters (0.65 μm Whatman) as described above for TPC, PON and TPP. Particulate silicate was leached from filtered material using 0.1 mol L⁻¹ NaOH at 85 °C for 2 h and 15 min, neutralised with H₂SO₄ (0.05 mol L⁻¹, Titrisol) and analysed as dissolved silicate by spectrophotometry according to Hansen and Koroleff (1999).

For further details about sediment trap powder analyses for TPP and BSi, see Boxhammer et al. (2015).

2.5.4 Dissolved organic matter (C, N, P)

For dissolved organic carbon (DOC) and total dissolved nitrogen (TDN) analyses, 35 mL of sample was filtered through pre-combusted GF/F filters (450 °C, 6 h) and collected in acid cleaned and combusted glass vials (450 °C, 6 h), acidified with HCl to pH 1.9 and then flame sealed, and dark-stored in a fridge (4 °C) for subsequent analysis. DOC and TDN concentrations were determined using a high-temperature catalytic combustion technique with a Shimadzu TOC-TN V analyser following Badr et al. (2003). Acidified deep Sargasso Sea water, preserved in glass ampoules and provided by D. Hansell (University of Miami), served as a certified reference material. Our analytical precision, based on the coefficient of variation (SD/mean) of consecutive measurements of a single sample (generally between 3 and 5 injections), was typically < 1 %. Dissolved organic nitrogen (DON) concentrations were calculated from TDN by the subtraction of the inorganic nitrogen concentrations.

Effect of elevated CO₂ on organic matter pools and fluxes in a summer

A. J. Paul et al.

Title Page

Abstract

Introduction

Conclusions

References

Tables

Figures

⏪

⏩

◀

▶

Back

Close

Full Screen / Esc

Printer-friendly Version

Interactive Discussion



Effect of elevated CO₂ on organic matter pools and fluxes in a summer

A. J. Paul et al.

Title Page

Abstract

Introduction

Conclusions

References

Tables

Figures



Back

Close

Full Screen / Esc

Printer-friendly Version

Interactive Discussion



Dissolved organic phosphorus (DOP) samples were collected as for DOC and TDN but stored at -20°C in acid-rinsed, high density polyethylene (HDPE) bottles. Total dissolved phosphate was decomposed to inorganic phosphate using an oxidising solution and microwave radiation (MARS 5X microwave, CEM) before analysis according to Hansen and Koroleff (1983). DOP concentrations were calculated from total dissolved phosphate by subtracting dissolved inorganic phosphate concentrations. Samples for DOP were only taken until $t30$. For further details, please refer to Nausch et al. (2015).

2.5.5 Phytoplankton pigments

Samples for fluorometric chlorophyll *a* determination (Chl *a*) and for phytoplankton pigment analyses by reverse phase high performance liquid chromatography (HPLC) were collected as described for POM with care taken to minimise exposure to light. Size fractionation for HPLC samples was achieved by pre-filtration using a $20\ \mu\text{m}$ mesh and $2\ \mu\text{m}$ membrane filters (Nuclepore) and was sampled for every 4th day, except for between $t31$ and $t39$ where sampling occurred only on $t31$, $t33$ and $t39$. Filtration volumes for the total and $< 2\ \mu\text{m}$ fraction as well as for Chl *a* were 500 mL whereas for the large fraction ($> 20\ \mu\text{m}$) volume ranged between 3000 and 5000 mL. All HPLC samples were stored at -80°C for under 6 months and Chl *a* samples at -20°C overnight until analysis.

Pigments from both fluorometric and HPLC analyses were extracted in acetone (90 %) in plastic vials by homogenisation of the filters using glass beads in a cell mill. After centrifugation (10 min, $800 \times g$, 4°C) the supernatant was analysed on a fluorometer (TURNER 10-AU) to determine Chl *a* concentrations (Welschmeyer, 1994). After centrifugation (10 min, 5200 rpm, 4°C), the supernatant was filtered through $0.2\ \mu\text{m}$ PTFE filters (VWR International). Phytoplankton pigment concentrations were determined in the supernatant by reverse phase high performance liquid chromatography (HPLC; WATERS HPLC with a Varian Microsorb-MV 100-3 C8 column; Barlow et al., 1997; Derenbach, 1969) and peaks were calibrated with the help of a library of pre-measured commercial standards. Relative contributions of phytoplankton groups to total Chl *a* were calculated using the CHEMTAX matrix factorisation program (Mackey

et al., 1996). Pigment ratios were adapted accordingly to those reported for Baltic Sea phytoplankton (Eker-Develi et al., 2008; Schluter et al., 2000; Zapata et al., 2000). The size fraction 2–20 μm was calculated as < 2 and > 20 μm subtracted from the total size fraction.

2.6 Statistical data treatment

As in previous mesocosm experiments, a $f\text{CO}_2$ gradient was chosen for reasons as outlined in Schulz et al. (2013). Linear regression analyses were used to determine the relationship between average $f\text{CO}_2$ and average response of the variables during each experimental phase. Outliers were detected based on Grubb's test ($p < 0.05$).

This test was applied to all treatments by experiment phase to account for temporal development of each variable. Detected outliers were not included in calculation of experiment phase average. Exceptions to outlier exclusion include (a) biogenic silicate concentrations in M8 on $t23$ because all data was higher on this particular sampling day, and (b) C:N in total POM on $t19$ in M8 because the C:N in this treatment was also markedly higher than other treatments on the following sampling day ($t21$) and (c) the contribution of cryptophytes to total Chl a M8 on $t17$ and (d) all five outliers in contribution of euglenophytes to total Chl a detected in Phase III for the same line of reasoning as (b). All data points are included in the figures with excluded outliers clearly marked. Linear regression analyses and outlier detection and exclusion were undertaken using R Project for Statistical Computing (<http://www.r-project.org/>).

3 Results

3.1 Variations in temperature, salinity and oceanographic conditions

Daily average water column temperature was highly variable over the experiment ranging from 8.0–8.5 $^{\circ}\text{C}$ at the beginning of the experiment to 16 $^{\circ}\text{C}$ on $t16$ (Fig. 5). Temperature variations as well as the first CO_2 manipulation on $t0$ were used to define

6877

BGD

12, 6863–6927, 2015

Effect of elevated CO_2 on organic matter pools and fluxes in a summer

A. J. Paul et al.

Title Page

Abstract

Introduction

Conclusions

References

Tables

Figures

◀

▶

◀

▶

Back

Close

Full Screen / Esc

Printer-friendly Version

Interactive Discussion



different experimental phases, (Phase 0 = $t-5$ to $t0$, Phase I = $t1$ to $t16$, Phase II = $t17$ to $t30$, Phase III = $t31$ to $t43$). Warming occurred over the first 15 days to peak at 16°C (Phase I). A cooling phase (Phase II) occurred until $t31$ ($\sim 8^\circ\text{C}$), followed by a second warming period (Phase III) which continued until the end of the experiment reaching around 12°C on average in the water column (Figs. 5 and 6c). The cooling in Phase II occurred around the same time as a period of lower incoming PAR between $t15$ and $t25$ (land based PAR measurements, Fig. 7a). Surface water temperatures reached a maximum of 18°C with a surface-to-depth gradient of 6°C . The water column in the mesocosms remained thermally stratified throughout the study according to daily CTD profiles. Stratification strength, defined here as the potential density anomaly (σ_T) difference between the surface 10 m and bottom 7 m above the sediment trap in each mesocosm, was variable but lower in Phase I than in II and III. Detected changes in density over time were largely driven by changes in temperature within the mesocosms as there was only a minimal increase in salinity during the experiment probably due to evaporation (Fig. 6, M8 as representative for all mesocosms). The increase in salinity on $t45$ is from addition of a calibrated salt solution for mesocosm volume determination. A notable decrease in temperature and increase in salinity in the archipelago between $t15$ and $t31$ coincided with a period of stormy weather and a change in wind direction from north-easterly to a more westerly direction, indicating a period of upwelling. During this period, there were slightly lower incoming PAR indicating higher cloud cover (Fig. 7). This depth of average light intensity was relatively stable between 3.7 and 4.7 m inside the mesocosms and very similar between treatments over time (Fig. 7).

3.2 Temporal variations in carbonate system

Before the first CO_2 enrichment on $t0$, all mesocosms had a similar pH_T of around 8.0. Initial CO_2 enrichment reached target values on $t4$ ranging from $\sim 240 \mu\text{atm}$ in the two ambient control mesocosms up to $\sim 1650 \mu\text{atm}$ in the highest treatment, corresponding to a pH_T range of ~ 7.45 to 8.2 (Fig. 8). Aside from the CO_2 addition on $t15$, $f\text{CO}_2$ was allowed to vary naturally and treatments remained well separated over the entire

BGD

12, 6863–6927, 2015

Effect of elevated CO_2 on organic matter pools and fluxes in a summer

A. J. Paul et al.

Title Page

Abstract

Introduction

Conclusions

References

Tables

Figures

◀

▶

◀

▶

Back

Close

Full Screen / Esc

Printer-friendly Version

Interactive Discussion



Effect of elevated CO₂ on organic matter pools and fluxes in a summer

A. J. Paul et al.

Title Page

Abstract

Introduction

Conclusions

References

Tables

Figures

◀

▶

◀

▶

Back

Close

Full Screen / Esc

Printer-friendly Version

Interactive Discussion



experiment. The decrease in $f\text{CO}_2$ over time in the high CO_2 treatment mesocosms was mostly driven by outgassing rather than biological uptake as productive biomass remained relatively low in this experiment (see Sect. 3.3). The effect of outgassing is evident in the rapid increase in surface pH_T in all treatment mesocosms (Fig. 9). Surrounding water pH_T (0–17 m) ranged from 8.30 initially to 7.75 during the experiment. The profound pH_T variability outside the mesocosms was due to upwelling of deeper, CO_2 -rich seawater. Within each mesocosm, CO_2 manipulations over the entire depth were relatively homogeneous initially. However a decrease in pH in the ambient control mesocosms below 5 m depth was detected from around $t15$ onwards, suggesting heterotrophic activity at depth involving respiration of organic matter to CO_2 (Fig. 9). DIC increased in the control mesocosms due to gas exchange, which counteracted losses through uptake by the plankton community which left the water column undersaturated in CO_2 compared to the overlying atmosphere ($\sim 230 \mu\text{atm}$ in control mesocosms vs. $\sim 400 \mu\text{atm}$ in atmosphere, Schernewski, 2011).

Calcium concentration was $2.17 \text{ mmol kg}^{-1}$ which was higher than calculated from a typical mean ocean salinity relationship of $1.67 \text{ mmol kg}^{-1}$ (Dickson et al., 2007), because of high riverine calcium carbonate inputs in the Baltic Sea (Feistel et al., 2010). We accounted for this in the calculation of the calcium carbonate saturation state in the water (Fig. 8d). All mesocosms apart from the two ambient controls during Phase 0 and I were undersaturated with respect to aragonite (Fig. 8d) and the highest three $f\text{CO}_2$ treatments were also undersaturated with respect to calcite (data not shown) during the entire experiment.

3.3 Effects of elevated CO_2

Out of 105 linear regressions applied to particulate and dissolved material from the water column and the accumulated sediment trap material to analyse the effect of CO_2 , we detected a significant correlation in 18. These are summarised in Table 3 and highlighted in the following sections. The majority of detected responses (14) indicated a positive effect of CO_2 whereas only four indicated a negative effect of CO_2 .

Effect of elevated CO₂ on organic matter pools and fluxes in a summer

A. J. Paul et al.

Title Page

Abstract

Introduction

Conclusions

References

Tables

Figures



Back

Close

Full Screen / Esc

Printer-friendly Version

Interactive Discussion



In this study, the low number of $f\text{CO}_2$ treatments (six) due to the exclusion of three mesocosms limits the statistical power of our conclusions. However the effect of CO_2 was consistent across biogeochemical element pools with higher sustained particulate matter concentrations and lower dissolved phosphate under high CO_2 . This gives us confidence that the results of our study are indicative of the response of this particular plankton community in the Baltic Sea to ocean acidification.

3.4 Chlorophyll *a* dynamics

An increase in Chl *a* began after $t1$ and signified a phase characterised by higher Chl *a* concentrations ($\sim 2 \mu\text{gL}^{-1}$) until $t16$ (Fig. 10, Phase I: $t1$ to $t16$). Chl *a* concentrations decreased by $\sim 0.8 \mu\text{gL}^{-1}$ in the mesocosms during Phase II and remained low and relatively stable in Phase III (~ 0.9 to $1.2 \mu\text{gL}^{-1}$). Between 50 and 80 % of Chl *a* was in the upper water column (IWS samples 0–10 m, Fig. 10c). Chl *a* concentrations were in general lower (0.9 to $2.5 \mu\text{gL}^{-1}$) in the mesocosms than in the surrounding water (1.2 to $5.5 \mu\text{gL}^{-1}$). CO_2 related differences among $f\text{CO}_2$ treatments first developed during Phase II and remained stable during Phase III with 24 % higher Chl *a* in the highest $f\text{CO}_2$ treatment in Phase III (Table 3).

3.5 Dissolved inorganic and organic matter dynamics

No inorganic nutrients were added to the mesocosms in this study. Thus, nutrient concentrations remained relatively stable with low inorganic nitrogen concentrations throughout the entire experiment. Concentrations were within the natural range for this region in a post-spring bloom phase (Fig. 11). There was low N ($\sim 50 \text{nmolL}^{-1}$ nitrate and $\sim 200 \text{nmolL}^{-1}$ ammonium) relative to phosphate ($\sim 150 \text{nmolL}^{-1}$) in all mesocosms compared to the canonical Redfield nutrient stoichiometry (Fig. 11, C:N:P = 106:16:1, Redfield (1958). Temporal dynamics between DIP and nitrate showed decoupling. Nitrate concentrations increased from $\sim 20 \text{nmolL}^{-1}$ up to $\sim 80 \text{nmolL}^{-1}$ from $t1$ until the end of the experiment ($t43$), whereas DIP concentrations

were slightly more dynamic. Around $t30$, differences in DIP between $f\text{CO}_2$ treatments became visible with a significant negative effect between $f\text{CO}_2$ and DIP concentration in Phase III (Table 3). For further details and discussion on phosphorus pool sizes, uptake rates and cycling, see Nausch et al. (2015).

Ammonium concentrations decreased from between ~ 170 and $\sim 280 \text{ nmol L}^{-1}$ on $t3$ to between 40 and 150 nmol L^{-1} on $t39$ with a small increase until $t43$ in all mesocosms (Fig. 11c). Samples for NH_4^+ concentration were lost on $t27$ and $t29$ for all mesocosms. The strongest decrease occurred during Phase I and concentrations remained relatively stable in Phase II and III. No significant $f\text{CO}_2$ effect was detected during any experimental phase above the variability in the data. Inside the mesocosms, dissolved silicate concentrations decreased minimally from around $6.2 \mu\text{mol L}^{-1}$ on $t1$ to between 5.5 and $5.8 \mu\text{mol L}^{-1}$ at the end of the initial productive Phase I on $t16$ (Fig. 11d). Thereafter, dissolved silicate remained relatively constant until the end of the experiment. No significant effect of $f\text{CO}_2$ on dissolved silicate concentrations was detected in any phase.

DOC concentrations ranged between 410 and $420 \mu\text{mol L}^{-1}$ on $t2$ and increased by $\sim 30 \mu\text{mol L}^{-1}$ up to between 440 and $450 \mu\text{mol L}^{-1}$ on $t43$ (Fig. 12a). In Phase III, DOC positively correlated with $f\text{CO}_2$ (Table 3). There was no statistically significant correlation of $f\text{CO}_2$ with DON or DOP concentrations in any experimental phase. No clear temporal trends were distinguished in DOP concentrations although DON decreased during Phase I (Fig. 12). Where data points are missing, DON could not be corrected for NH_4^+ concentrations hence are excluded from the data set.

3.6 Particulate matter dynamics

Particulate C, N and P concentrations generally mirrored Chl a dynamics (Fig. 13) and were higher in Phase I than in Phase II and III for both size fractions in TPC (TPC_{tot}, Fig. 13a; TPC_{<55}, data not shown). The majority of particulate organic carbon and nitrogen was present in POM_{<55}. The importance of small particles was even more pronounced in Phase III, where in all mesocosms up to 90 % of total particulate organic

BGD

12, 6863–6927, 2015

Effect of elevated CO_2 on organic matter pools and fluxes in a summer

A. J. Paul et al.

Title Page

Abstract

Introduction

Conclusions

References

Tables

Figures

◀

▶

◀

▶

Back

Close

Full Screen / Esc

Printer-friendly Version

Interactive Discussion



matter was attributed to the fraction $\text{TPC}_{<10}$ (data not shown). In Phase III, there was a significant positive correlation between $f\text{CO}_2$ and average total TPC, PON and TPP (see Table 3).

C:N and C:P ratios in POM_{tot} (Fig. 14) were above the Redfield ratio (C:N:P_{tot} = 106:16:1) during the productive phase, peaked at the beginning of Phase I (C:N_{tot} = 7–8.5, C:P_{tot} = 110–160) then decreased and became stable during Phase II (C:N_{tot} = 5.8–7.0, C:P_{tot} = 80–140). C:N in $\text{POM}_{<55}$ remained stable and close to, or slightly higher than the Redfield ratio during the entire experiment (range of 6.5 to 9.2, see Fig. 15). Differences between $f\text{CO}_2$ treatments were first observed in Phase III with higher C:N_{tot} and C:N_{<55} in the highest $f\text{CO}_2$ treatment. No significant effect of $f\text{CO}_2$ on N:P or C:P was detected in any experiment phase or in any size fraction.

BSi decreased from around $1.0 \mu\text{molL}^{-1}$ at the beginning to $\sim 0.3 \mu\text{molL}^{-1}$ at the end of the experiment (Fig. 13). During Phase II, there was a statistically significant correlation of BSi with $f\text{CO}_2$, however this was absent in Phases I and III (Table 3).

3.7 Phytoplankton succession

The contribution to Chl *a* by different phytoplankton groups varied over time although the temporal trends in all mesocosms were remarkably similar (Fig. 16). Results from CHEMTAX analyses of the phytoplankton community present indicate that cryptophytes and chlorophytes had the highest contribution to total Chl *a* during Phase I and Phase II/III, respectively. The total abundances of cryptophytes decreased from *t*3 to *t*17 in all mesocosms, succeeded by a brief euglenophyte peak around *t*15, with chlorophytes being the dominant contributor to Chl *a* from *t*17 on (Fig. 16). Total abundances of cyanobacteria, probably non-diazotrophic *Synechococcus*, was highest during Phase III. Diatoms made up a relatively small proportion of the plankton assemblage and contributed to less than 10% of Chl *a* in Phases I and II and between 10–25% in Phase III. Other key groups detected included dinoflagellates and prasin-

BGD

12, 6863–6927, 2015

Effect of elevated CO_2 on organic matter pools and fluxes in a summer

A. J. Paul et al.

Title Page

Abstract

Introduction

Conclusions

References

Tables

Figures

⏪

⏩

◀

▶

Back

Close

Full Screen / Esc

Printer-friendly Version

Interactive Discussion



phytes, however, they made up minor proportions (below 15% of total Chl *a*) of the plankton community throughout the entire experiment (dinoflagellate data not shown).

We analysed the relationship between $f\text{CO}_2$ and the contribution of phytoplankton groups to Chl *a* by linear regression for each experimental phase (Table 4). These analyses indicated small differences in plankton community composition between CO_2 treatments. There was a significant negative correlation between CO_2 and total diatom contribution to Chl *a* in Phase III. In Phase III, $f\text{CO}_2$ was also negatively correlated to the contribution of cryptophytes to Chl *a* and a significant positive effect on the contribution of prasinophytes to Chl *a*.

Linear regression of the absolute concentrations of a number of phytoplankton pigments in the size fraction $< 2\ \mu\text{m}$ indicated primarily a positive correlation to $f\text{CO}_2$ during Phase I (i.e. Chl *a*, Violaxanthin, Neoxanthin) although a statistically significant effect was not detected in all pigments (Table 5). A positive correlation between picoeukaryote abundance and CO_2 treatment was also already detected in Phase I (Crawford et al., 2015). Absolute concentrations of Chl *a*, Chl *b*, Prasinolaxanthin, Violaxanthin and Neoxanthin in the total fraction had a statistically significant positive correlation with $f\text{CO}_2$ during Phase III (see Table 5). Fucoxanthin concentrations (diatom marker pigment but also present in dinoflagellates) and $f\text{CO}_2$ were also positively correlated in the fraction $> 20\ \mu\text{m}$ during Phase III. Size fractionation of HPLC pigment analyses indicated a higher proportion of Chl *a* in all treatments in biomass $< 2\ \mu\text{m}$ during Phases II and III (Fig. 17).

3.8 Sinking material flux

The amount of material collected in the sediment traps in each phase reflected biomass (here POM and Chl *a*) build-up from the water column. We calculated that $> 84\%$ of total carbon sinking into the sediment trap was collected during Phases I and II and less than 16% during Phase III (see Fig. 18). This corresponds to average accumulation rates ($\pm\text{SD}$) of 0.303 ± 0.011 , 0.203 ± 0.033 and $0.094 \pm 0.029\ \mu\text{mol CL}^{-1}\ \text{day}^{-1}$ across all mesocosms in Phases I, II and III respectively. No significant CO_2 trends

BGD

12, 6863–6927, 2015

Effect of elevated CO_2 on organic matter pools and fluxes in a summer

A. J. Paul et al.

Title Page

Abstract

Introduction

Conclusions

References

Tables

Figures

◀

▶

◀

▶

Back

Close

Full Screen / Esc

Printer-friendly Version

Interactive Discussion



were detected during any phase with regards to the total amount of C, N, P and BSi in the sediment trap material.

4 Discussion

4.1 Temporal dynamics in physical and chemical parameters and phytoplankton biomass

Conditions in the Tvärminne Storfjärden at the beginning of the experiment and during mesocosm closure were typical for a post spring-bloom phase in the early summer season. Daily solar irradiance was at the annual peak with relatively low nitrate concentrations, undersaturation of CO₂, surface water temperatures around ~ 10°C and relatively low Chl *a* of about 1.5 µg L⁻¹ (Figs. 5, 8 and 10). These post spring-bloom conditions were the same in all treatments. As is common in the Baltic Sea following the spring bloom (Matthäus et al., 1999), there was a large excess of dissolved inorganic phosphate (inorganic nutrient N : P ~ 1.25 : 1, Redfield N : P = 16 : 1) and relatively high concentrations of dissolved silicate (Fig. 11d). Fixed nitrogen availability primarily limited development of phytoplankton biomass in this system. For further discussion of the nitrogen cycle in this experiment, see Paul et al. (2015).

In the mesocosms, a gradual increase in CO₂ in the ambient treatments during the study period indicated ingassing of CO₂ as the water column was undersaturated with a likely contribution of organic matter remineralisation in the lower mesocosm (see Sect. 4.3 for further discussion). The C : N ratio of POM decreased slightly to be closer to Redfield ratio during the productive Phase I suggesting that N-rich organisms such as zooplankton and new phytoplankton biomass made up an increasing part of the POM pool during this period.

Microscopy counts revealed no significant bloom development of filamentous diazotrophic cyanobacteria in this study (A. Stühr, personal communication, 2014) although conditions generally fitted the widely regarded niche for this functional group

BGD

12, 6863–6927, 2015

Effect of elevated CO₂ on organic matter pools and fluxes in a summer

A. J. Paul et al.

Title Page

Abstract

Introduction

Conclusions

References

Tables

Figures

⏪

⏩

◀

▶

Back

Close

Full Screen / Esc

Printer-friendly Version

Interactive Discussion



Effect of elevated CO₂ on organic matter pools and fluxes in a summer

A. J. Paul et al.

Title Page

Abstract

Introduction

Conclusions

References

Tables

Figures



Back

Close

Full Screen / Esc

Printer-friendly Version

Interactive Discussion



in the Baltic Sea (excess inorganic phosphate, increasingly stratified water column, Vahtera et al., 2007). A strong, wind-driven upwelling event in the surrounding seawater occurred between $t15$ and $t23$ and brought cooler, more saline water from the Gulf of Finland into the study area (salinity profile, Fig. 6). Upwelling events are known to occur in the region (Kahru et al., 1995; Lips and Lips, 2010) particularly during south-westerly winds and have a considerable influence on the ecosystem productivity (Nõmmann et al., 1991). Temperature decreases of greater than 10°C in surface water temperature, as we observed in this study, have been reported for upwelling events during periods of thermal stratification (Lehmann and Myrberg, 2008). This change in temperature had a notable effect both in the archipelago and inside the mesocosms, likely decreasing plankton growth rates. In addition to the temperature decrease, there was a lower daily PAR flux around $t15$, therefore average light exposure for phytoplankton was reduced around this time (Fig. 7a). Thus, the large temperature fluctuations most likely played a central role in modulating temporal variations in autotrophic biomass and additionally likely muted development of diazotrophic cyanobacteria during the cooler phase in the middle of the experiment (Mehnert et al., 2010).

Despite the isolation of the communities in each mesocosm and the water mass variability outside the mesocosms, Chl a concentrations decreased simultaneously both inside and outside the mesocosms after $t16$. In addition, patterns in phytoplankton succession were similar (Figs. 10 and 16, Baltic Sea phytoplankton pigment concentrations are not shown because of different scale required). Dominance of Chlorophyceae in the phytoplankton community increased with decreasing temperature during Phase II at the expense of Euglenophyceae consistently across all mesocosms (CHEMTAX analyses, Fig. 16). The magnitude of change was higher outside the mesocosms than inside (eg. Chl a 2.5 times greater, Fig. 10a) because of water mass exchange and entrainment of nutrients. Unlike the water surrounding them where upwelling can bring water masses with different nutrient concentrations and different plankton populations, the mesocosms are closed structures. Hence, it appears that the plankton community itself is deterministic through natural succession. Here, low nutrient concentrations in

the mesocosms capped total biomass rather than having a strong influence on plankton community structure.

In the following three sections, the correlation between temperature and organic matter pools in the three experimental phases will be discussed, highlighting the presence and relevance of potential CO₂ effects.

4.2 Phase I: productive phase with high organic matter turnover

Phase I (*t1* to *t16*) was characterised by the highest sustained Chl *a* and particulate matter concentrations in the water column. Relatively high light availability, particularly between *t6* and *t15* (Fig. 7a), accompanied by increasing water column temperatures supported autotrophic growth. However, no increase in particulate matter pool size was observed in any treatment during this productive phase. DON, DIP and DSi concentrations seemed to decrease during this productive phase indicating net utilisation of organic nitrogen and inorganic phosphorus to maintain phytoplankton growth under low inorganic nitrogen concentrations. In general, dissolved organic nutrient concentrations were considerably higher compared to open ocean concentrations (this study = ~ 20–25 μmol L⁻¹, North Atlantic Ocean = 5–12 μmol L⁻¹, Torres-Valdés et al., 2009) but within the range of reported values for this part of the Gulf of Finland (up to 38.5 μmol L⁻¹, Hoikkola, 2012). Accumulation rates of total carbon in the sediment trap during Phase I indicate higher sinking flux in this period compared to Phases II and III. In addition to the high sinking flux strength, fixed carbon was also channelled into the DOC pool (Fig. 12) with a daily accumulation of between 10 to 15 % of the total TPC pool between *t3* and *t13*. As inorganic nitrogen availability was very low, we assume this is due to carbon overconsumption (Toggweiler, 1993). Thus, it appears as though organic matter turnover in the system was high during this period, although overall phytoplankton biomass production was limited by low inorganic nitrogen availability.

During the productive period in Phase I, we detected no statistically significant differences in bulk organic matter concentrations or elemental stoichiometry between CO₂ treatments. Instead, detected differences between *f*CO₂ treatments in particulate or

BGD

12, 6863–6927, 2015

Effect of elevated CO₂ on organic matter pools and fluxes in a summer

A. J. Paul et al.

Title Page

Abstract

Introduction

Conclusions

References

Tables

Figures

⏪

⏩

◀

▶

Back

Close

Full Screen / Esc

Printer-friendly Version

Interactive Discussion



dissolved matter were mostly confined to pigment concentrations in the smallest size fraction (< 2 µm). Here, pigment concentrations were generally higher in the highest CO₂ treatment (Table 5). This is in line with flow cytometry counts which revealed a positive effect of CO₂ on the abundance of picoeukaryotes (Crawford et al., 2015) and is in agreement with studies in both the high Arctic (Brussaard et al., 2013), the sub-arctic North Pacific (Endo et al., 2013), and North Atlantic Ocean (Newbold et al., 2012) but contrasts the results from Richier et al. (2014) from shelf seas in north-western Atlantic Ocean. The positive influence of CO₂ on phytoplankton pigment concentrations was also detected in the largest size fraction (> 20 µm) in Phase I, however made up only a small portion of total Chl *a* (< 10% Fig. 17, size fractionated pigment analyses). In this phase, phytoplankton between 2–20 µm in size, primarily Euglenophytes, made up between 25 and 65 % of Chl *a*.

Although phytoplankton carbon fixation is expected to be stimulated by increased CO₂ availability (Hein and Sand-Jensen, 1997; Losh et al., 2012; Riebesell et al., 2007), previous CO₂ enrichment experiments using natural plankton assemblages under various conditions of nutrient repletion in different regions have shown no consistent response of primary production to elevated CO₂ (Engel et al., 2005; Hopkins et al., 2010; Hopkinson et al., 2010; Nielsen et al., 2011; Riebesell et al., 2007; Schulz et al., 2015; Yoshimura et al., 2013). During high organic matter turnover in Phase I, no CO₂ signal could be detected in the most abundant, and presumably most productive, phytoplankton size class. Thus, small differences in plankton community structure in the smallest and largest phytoplankton driven by CO₂ were not relevant for biogeochemical element cycling in this plankton assemblage during this productive phase.

4.3 Phase II: temperature induced decline in autotrophic productivity

In Phase II, average water column temperature decreased by ~ 8 °C and incoming PAR was comparatively lower until *t*24. We suggest this slowed down phytoplankton productivity and contributed to the sharp decline in Chl *a* concentrations in all mesocosms and the surrounding Baltic Sea between *t*17 and *t*27 (Fig. 10). While the temperature

Effect of elevated CO₂ on organic matter pools and fluxes in a summer

A. J. Paul et al.

[Title Page](#)[Abstract](#)[Introduction](#)[Conclusions](#)[References](#)[Tables](#)[Figures](#)[Back](#)[Close](#)[Full Screen / Esc](#)[Printer-friendly Version](#)[Interactive Discussion](#)

decrease occurred concurrently with Chl *a* decline both inside and outside the mesocosms, different mechanisms are responsible for this decrease. For example, outside the mesocosms upwelling of low Chl *a* water may have diluted the surface concentration and increased light availability in the water column, whereas inside the sealed mesocosms this is was not the case.

DOC and DON concentrations also remained relatively stable during the decrease in Chl *a*, thus suggesting that carbon fixation fuelled by DON utilisation was considerably lower than in Phase I. Although there was a marked decrease in Chl *a* after *t17*, TPC concentration remained relatively stable and was reflected in an increase in $TPC_{tot} : Chl\ a$ from $\sim 10\ \mu\text{mol}\ \mu\text{g}^{-1}$ on *t17* to over $15\ \mu\text{mol}\ \mu\text{g}^{-1}$ on *t29*. Both ratios are in a range expected for a mixed plankton community in the Tvärminne area (Spilling et al., 2014). This increase in $TPC_{tot} : Chl\ a$ indicates that carbon was being shifted from primary producers to zooplankton and other non-chlorophyll containing organisms or that the background TPC was high with a declining contribution of fresh phytoplankton biomass to particulate carbon.

Indeed, zooplankton abundances increased profoundly between *t17* and *t31* as reported by Lischka et al. (2015). Warmer temperatures up until *t17* probably enhanced zooplankton reproduction rates during Phase I and hence also grazing pressure in Phase II. The combination of higher grazing pressure, lower PAR and cooler temperatures likely contributed to decreased phytoplankton biomass, observed here as a decrease in Chl *a*, during Phase II (*t17* to *t30*). Correspondingly, less material was collected in the sediment trap during Phase II, where autotrophic biomass and the average phytoplankton size, determined by size-fractionated Chl *a* concentrations, decreased. By the end of the decline in Chl *a* in the water column on *t30*, approximately 85 % of total sinking material collected over the full duration of the experiment had collected in the sediment trap.

The vertical distribution of Chl *a* in the water column also correlated to temperature fluctuations. As expected, the majority of Chl *a* was contained in the top 10 m of the water column (Fig. 10c) where light intensity was considerably higher. At the

BGD

12, 6863–6927, 2015

Effect of elevated CO₂ on organic matter pools and fluxes in a summer

A. J. Paul et al.

Title Page

Abstract

Introduction

Conclusions

References

Tables

Figures

◀

▶

◀

▶

Back

Close

Full Screen / Esc

Printer-friendly Version

Interactive Discussion



Effect of elevated CO₂ on organic matter pools and fluxes in a summer

A. J. Paul et al.

Title Page

Abstract

Introduction

Conclusions

References

Tables

Figures



Back

Close

Full Screen / Esc

Printer-friendly Version

Interactive Discussion



same time as surface Chl *a* (0 to 10 m) decreased between *t*18 and *t*30, CTD profiles showed a decrease in pH_T below 10 m in both control mesocosms (Fig. 9). This pH decrease could indicate a possible change in the equilibrium between dominance of autotrophic (DIC uptake) to heterotrophic (DIC release) processes during a phase of strong cooling in the lower water column. In addition, pH decrease from an increase in net heterotrophy must have been strong enough to compensate for the increase in pH due to the change in carbonate system equilibrium with the temperature decrease (Gieskes, 1969). However, there are a few factors which could potentially explain this observation. Firstly, higher organic material availability seemed to stimulate bacterial activity up until *t*23 (Nausch et al., 2015). A concurrent reduction in PAR would have also diminished autotrophic activity particularly in the lower water column in the mesocosms thereby supporting net heterotrophy at depth. Furthermore, higher zooplankton abundances after *t*17 (Lischka et al., 2015) as well as a peak in abundance of a potential mixotroph around *t*17 (Euglenophyceae) also likely contributed to higher remineralisation and DIC release. Due to *f*CO₂ manipulations in all other treatments, pH changes due to heterotrophic activity could not be distinguished from the overall outgassing trend but changes were likely present underneath the overriding CO₂ signal. Hence Phase II is defined by increased heterotrophy and organic matter remineralisation, where carbon was primarily channelled into sinking material flux and higher trophic levels rather than the DOC pool, mediated by increased zooplankton grazing pressure on primary producers.

During the Chl *a* decrease, we observed differences between CO₂ treatments in the dissolved and particulate matter pools. In addition, size-fractionated pigment analyses indicate that up to ~ 90 % of Chl *a* was in phytoplankton < 2 μm at the end of Phase II. This was not due to an increase in Chl *a* in the smaller size class but rather due to zooplankton grazing and the temperature decrease which together selectively acted to remove the larger size classes. This selective removal then revealed the underlying CO₂ response of picoplankton that was already present since Phase I. This is further supported by particulate matter C : N_{tot} ratios in different size fractions, where the

Effect of elevated CO₂ on organic matter pools and fluxes in a summer

A. J. Paul et al.

Title Page

Abstract

Introduction

Conclusions

References

Tables

Figures

◀

▶

◀

▶

Back

Close

Full Screen / Esc

Printer-friendly Version

Interactive Discussion



C : N_{tot} became more similar to the C : N_{<10} towards the end of Phase II. In other words, a positive CO₂ effect on picophytoplankton seemed to be present throughout the entire experiment. However, their ecological and biogeochemical relevance within the plankton community was too small initially, so that the CO₂ effect was not detectable in the other bulk variables.

Interestingly, measured carbon fixation rates did not show any fertilising effect of CO₂ (Spilling et al., 2015), whereas both respiration (Spilling et al., 2015) and bacterial production rates between *t*14 and *t*23 (Nausch et al., 2015) were lower at higher CO₂. This suggests slower net particulate matter loss rather than increased production under ocean acidification (see Spilling et al. (2015) and Nausch et al. (2015) in this issue for more thorough discussion on this topic).

4.4 Phase III: inactive plankton community

While temperature increased again during Phase III, there did not seem to be any revival of phytoplankton productivity to the same level as in Phase I. In Phase II autotrophic growth was apparently dampened so severely that it could not recover within the duration of this study and was likely strongly controlled by high zooplankton grazing pressure. There was very little change in the amount or stoichiometry of the particulate or dissolved matter pools suggesting that production and loss of particulate matter in the water column were relatively well balanced in Phase III. Only a small amount ($\sim 1 \mu\text{mol L}^{-1}$) of TPC was collected in the sediment traps implying low particulate matter sinking flux strength in this phase. The positive effect of CO₂ on particulate and dissolved pools unmasked in Phase II was sustained throughout Phase III in Chl *a*, TPC, PON, TPP and DIP due to the continued dominance of picophytoplankton. Thus in this study, higher autotrophic biomass was sustained under elevated CO₂ in this plankton community during the post-bloom phase and had a significant influence on biogeochemical pool sizes.

Yet, variations in water column particulate matter concentrations did not translate into statistically significant differences in the amount of accumulated sediment trap mate-

Effect of elevated CO₂ on organic matter pools and fluxes in a summer

A. J. Paul et al.

Title Page

Abstract

Introduction

Conclusions

References

Tables

Figures



Back

Close

Full Screen / Esc

Printer-friendly Version

Interactive Discussion



rial between CO₂ treatments. Differences in sinking flux between treatments may have been too small or the experiment time scale too short to resolve any effect of CO₂. However, the positive effect of CO₂ on particulate matter pools was reflected positively in the DOC pool suggesting that a higher proportion of organic matter was directed
 5 into the microbial food web, rather than being exported during the period of low organic matter turnover in Phase III. This was probably because the response of CO₂ was the strongest in phytoplankton < 2 μm, which taxonomically are likely to be chlorophytes and prasinophytes (Fig. 16b and f, Table 4). The picophytoplankton present were too small to sink as individual cells or to be directly ingested by copepods (Sommer et al., 2002). In order to sink, picoplankton cells must aggregate or be consumed by zooplankton. Cell aggregates can be consumed and repackaged by zooplankton into larger particles and thereby can indirectly have a significant contribution to carbon export (Richardson and Jackson, 2007). Based on our results, we hypothesise that under future ocean acidification the Baltic Sea in low nitrogen, summer periods may shift
 10 towards a system where more organic matter is retained in the upper water column but will not result in increased particulate matter flux. This could be of particular relevance for the oxygen budget in the Baltic Sea, with reduced oxygen consumption in bottom waters. This does not support the suggestion by Jutterström et al. (2014) that ocean acidification might exacerbate already high organic matter production in the surface due to eutrophication and thereby further increase oxygen consumption in the deeper basins in the Baltic Sea when it sinks below the halocline.

4.5 Potential ecosystem resilience under elevated CO₂

The Baltic Sea is a highly dynamic system with much larger annual temperature, light period, inorganic nutrient, pH, and salinity fluctuations than in many other major water
 25 bodies and the open ocean. While a significant, but small, response to CO₂ was detected in a number of particulate and dissolved matter pools, in numerous others no significant effect of CO₂ was detected in any phase (e.g. DON and DOP concentration, N:P and C:P in POM, Table 5). In the Tvärminne Storfjärden, pH varies markedly

both diurnally (~ 0.1 during summer, Almén et al., 2014) and seasonally (~ 0.6 winter vs. summer, Brutemark et al., 2011), particularly due to high variability in primary productivity and temperature as well as upwelling events. Within this study period, upwelling into the Storfjärden brought cold, CO_2 -rich deep water to the surface. $f\text{CO}_2$ in the surrounding water ranged from ~ 240 to $\sim 800 \mu\text{atm}$ on $t33$ corresponding to a pH_T drop of ~ 0.5 units. Thus the muted response to CO_2 that we observed in this experiment in a number of parameters could be linked to higher tolerance or resilience of the plankton community due to physiological plasticity through exposure to large natural diurnal and annual fluctuations in carbonate chemistry speciation and pH (see also Joint et al. (2011) and Nielsen et al., 2011). In past CO_2 enrichment experiments, nutrient addition amplified the existing effect of CO_2 between treatments, for example Schulz et al. (2013). Hence low nitrogen availability in this study may have dampened underlying trends particularly in larger phytoplankton size classes.

5 Conclusions

Large fluctuations in temperature correlated well to Chl *a* concentrations and community size structure in all treatments. Thus temperature fluctuations were used to define three experiment phases after CO_2 manipulation. Increased temperature and higher PAR during Phase I ($t1$ to $t16$) supported autotrophic development and sustained higher organic matter sinking fluxes. Around $t17$ an upwelling event was induced by a change in wind direction, reduced PAR through greater cloud cover and cooled the water column. In Phase II ($t17$ to $t30$), higher grazing pressure from zooplankton combined with water column cooling initiated the loss of phytoplankton biomass which we observed as a decrease in Chl *a*. Phase III ($t31$ to $t43$) was defined as a warming phase characterised by stable particulate matter concentrations, increased proportion of nutrient regeneration in the water column and low sinking material fluxes.

It is likely that the muted response of the plankton community and biogeochemistry in this experiment to elevated $f\text{CO}_2$ is due to a combination of high natural variability in

Effect of elevated CO_2 on organic matter pools and fluxes in a summer

A. J. Paul et al.

Title Page

Abstract

Introduction

Conclusions

References

Tables

Figures



Back

Close

Full Screen / Esc

Printer-friendly Version

Interactive Discussion



Effect of elevated CO₂ on organic matter pools and fluxes in a summer

A. J. Paul et al.

[Title Page](#)[Abstract](#)[Introduction](#)[Conclusions](#)[References](#)[Tables](#)[Figures](#)[Back](#)[Close](#)[Full Screen / Esc](#)[Printer-friendly Version](#)[Interactive Discussion](#)

$f\text{CO}_2$ in the system and limited nitrogen availability and no significant development of a summer cyanobacteria bloom. However where effects of $f\text{CO}_2$ were detected, they were consistent across the biogeochemical pools and in agreement with results from previous ocean acidification ecosystem studies in a variety of regions. A significant positive effect of $f\text{CO}_2$ on picophytoplankton ($< 2\ \mu\text{m}$) biomass was detected during Phase I, although no significant differences in bulk particulate or dissolved matter pools were observed during this period. No effect of CO_2 was identified in larger organisms (2 to $20\ \mu\text{m}$) which were dominant in the phytoplankton community during Phase I. Hence their dominance masked the CO_2 signal from picophytoplankton. The potentially positive effect of CO_2 on community Chl *a* and particulate material concentrations became evident towards the end of Phase II when the size structure of the phytoplankton community shifted towards a dominance of smaller phytoplankton size classes. As a result, the underlying positive effect of CO_2 present since Phase I was revealed. However this signal could not be explained by a detectable increase in carbon fixation in this study (see also Spilling et al., 2015). Instead higher organic matter concentration is more likely due to decreased net respiration at higher $f\text{CO}_2$. Thus it appears that CO_2 modulated the coupling between autotrophic and heterotrophic processes, particularly during loss of phytoplankton biomass. During Phase III, picoplankton contributed up to $\sim 90\%$ of total Chl *a*. In this phase, we observed higher post-bloom Chl *a*, particulate organic matter and DOC concentrations at elevated $f\text{CO}_2$ in this nitrogen-limited plankton community, driven by the response of picophytoplankton.

Consequently, differences in water column biomass did not directly translate into increased particle sinking flux at higher $f\text{CO}_2$. Picophytoplankton are too small to sink as individual cells thus when they were dominant in the plankton community during the regenerative period (Phase III), particulate organic material reworking and repackaging by zooplankton instead mediated sinking flux. This secondary processing of sinking material likely removed the CO_2 signal present in the water column particulate matter so that it was not reflected in the collected sinking material during the study period. Hence we suggest CO_2 -induced changes in productivity in the upper water column

may be decoupled from particle sinking flux and potentially oxygen consumption below the euphotic layer in the Baltic Sea.

This is one of few plankton community experiments, where nutrient concentrations were very low initially and concentrations and nutrient ratios were not manipulated.

5 These conditions are representative of a steady-state stratified water column present in many ecosystems for most of the year. We first observed CO₂-related differences in bulk biogeochemical pools after almost four weeks. Therefore we suggest future experiments should run for as long as practically feasible and focus on the vast oligotrophic regions and not include any nutrient addition to confirm speculations on how these low
10 nutrient, less productive ecosystems will react to future ocean acidification. Changes in the abundance of key phytoplankton groups in steady-state systems due to higher CO₂ may underpin sustained fundamental changes in biogeochemical cycling in these regions.

15 *Acknowledgements.* We thank the KOSMOS team and all of the participants in the mesocosm campaign for their support during the experiment. In particular, we would like to thank Andrea Ludwig for co-ordinating the campaign logistics and assistance with CTD operations, the diving team, as well as Kerstin Nachtigall for analyses, and Josephine Goldstein, Mathias Haunost, Francois Legiret, Jana Meyer, Michael Meyerhöfer, and Jehane Ouriqua for assistance in sampling and analyses, Annegret Stuhr for helpful discussions, and Regina Surberg for
20 calcium analyses. We would also like to sincerely thank the Tvärminne Zoological Station for their warm hospitality, support and use of facilities for this experiment. We also gratefully acknowledge the captain and crew of R/V *ALKOR* for their work transporting, deploying and recovering the mesocosms. This collaborative project was funded by Cluster of Excellence “The Future Ocean” (Project CP1141) and by BMBF projects BIOACID II (FKZ 03F06550), SOPRAN Phase II (FKZ 03F0611), and MESOAQUA (grant agreement number 228224).
25

The article processing charges for this open-access publication were covered by a Research Centre of the Helmholtz Association.

Effect of elevated CO₂ on organic matter pools and fluxes in a summer

A. J. Paul et al.

Title Page

Abstract

Introduction

Conclusions

References

Tables

Figures



Back

Close

Full Screen / Esc

Printer-friendly Version

Interactive Discussion



References

- Almén, A.-K., Vehmaa, A., Brutemark, A., and Engström-Öst, J.: Coping with climate change? Copepods experience drastic variations in their physicochemical environment on a diurnal basis, *J. Exp. Mar. Biol. Ecol.*, 460, 120–128, doi:10.1016/j.jembe.2014.07.001, 2014.
- 5 Badr, E.-S. A., Achterberg, E. P., Tappin, A. D., Hill, S. J., and Braungardt, C. B.: Determination of dissolved organic nitrogen in natural waters using high-temperature catalytic oxidation, *TrAC-Trend. Anal. Chem.*, 22, 819–827, doi:10.1016/S0165-9936(03)01202-0, 2003.
- Barlow, R. G., Cummings, D. G., and Gibb, S. W.: Improved resolution of mono- and divinyl chlorophylls *a* and *b* and zeaxanthin and lutein in phytoplankton extracts using reverse phase
10 C-8 HPLC, *Mar. Ecol.-Prog. Ser.*, 161, 303–307, doi:10.3354/meps161303, 1997.
- Biswas, H., Gadi, S. D., Ramana, V. V., Bharathi, M. D., Priyan, R. K., Manjari, D. T., and Kumar, M. D.: Enhanced abundance of tintinnids under elevated CO₂ level from coastal Bay of Bengal, *Biodivers. Conserv.*, 21, 1309–1326, doi:10.1007/s10531-011-0209-7, 2012.
- Boxhammer, T. et al.: *Biogeosciences*, in preparation, 2015.
- 15 Brussaard, C. P. D., Noordeloos, A. A. M., Witte, H., Collenteur, M. C. J., Schulz, K., Ludwig, A., and Riebesell, U.: Arctic microbial community dynamics influenced by elevated CO₂ levels, *Biogeosciences*, 10, 719–731, doi:10.5194/bg-10-719-2013, 2013.
- Brutemark, A., Engström-Öst, J., and Vehmaa, A.: Long-term monitoring data reveal pH dynamics, trends and variability in the western Gulf of Finland, *Oceanol. Hydrobiol. St.*, 40, 91–94, doi:10.2478/s13545-011-0034-3, 2011.
- 20 Calbet, A., Sazhin, A. F., Nejstgaard, J. C., Berger, S. A., Tait, Z. S., Olmos, L., Sousoni, D., Isari, S., Martínez, R. A., Bouquet, J.-M., Thompson, E. M., Båmstedt, U., and Jakobsen, H. H.: Future climate scenarios for a coastal productive planktonic food web resulting in microplankton phenology changes and decreased trophic transfer efficiency, *PLoS ONE*, 9, e94388, doi:10.1371/journal.pone.0094388, 2014.
- 25 Crawford, K. et al.: *Biogeosciences*, in preparation, 2015.
- Czerny, J., Schulz, K. G., Krug, S. A., Ludwig, A., and Riebesell, U.: Technical Note: The determination of enclosed water volume in large flexible-wall mesocosms "KOSMOS", *Biogeosciences*, 10, 1937–1941, doi:10.5194/bg-10-1937-2013, 2013.
- 30 Derenbach, J.: Zur Homogenisation des Phytoplanktons für die Chlorophyllbestimmung, *Kieler Meeresforschungen*, 25, 166–171, 1969.

Effect of elevated CO₂ on organic matter pools and fluxes in a summer

A. J. Paul et al.

Title Page

Abstract

Introduction

Conclusions

References

Tables

Figures



Back

Close

Full Screen / Esc

Printer-friendly Version

Interactive Discussion



Effect of elevated CO₂ on organic matter pools and fluxes in a summer

A. J. Paul et al.

Title Page

Abstract

Introduction

Conclusions

References

Tables

Figures



Back

Close

Full Screen / Esc

Printer-friendly Version

Interactive Discussion



- Dickson, A.: An exact definition of total alkalinity and a procedure for the estimation of alkalinity and total inorganic carbon from titration data, *Deep-Sea Res.*, 28, 609–623, 1981.
- Dickson, A. G.: Standards for ocean measurements, *Oceanography*, 23, 34–47, doi:10.5670/oceanog.2010.22, 2010.
- 5 Dickson, A. G., Sabine, C., and Christian, J. (Eds.): Guide to Best Practices for Ocean CO₂ Measurements, PICES Special Publication 3, 191 pp., <http://aquaticcommons.org/1443/>, 2007.
- Doney, S. C., Mahowald, N., Lima, I., Feely, R. A., Mackenzie, F. T., Lamarque, J.-F., and Rasch, P. J.: Impact of anthropogenic atmospheric nitrogen and sulfur deposition on ocean acidification and the inorganic carbon system, *P. Natl. Acad. Sci. USA*, 104, 14580–14585, doi:10.1073/pnas.0702218104, 2007.
- 10 Dore, J. E., Lukas, R., Sadler, D. W., Church, M. J., and Karl, D. M.: Physical and biogeochemical modulation of ocean acidification in the central North Pacific, *P. Natl. Acad. Sci. USA*, 106, 12235–12240, doi:10.1073/pnas.0906044106, 2009.
- 15 Ekau, W., Auel, H., Pörtner, H.-O., and Gilbert, D.: Impacts of hypoxia on the structure and processes in pelagic communities (zooplankton, macro-invertebrates and fish), *Biogeosciences*, 7, 1669–1699, doi:10.5194/bg-7-1669-2010, 2010.
- Eker-Develi, E., Berthon, J.-F., and Van der Linde, D.: Phytoplankton class determination by microscopic and HPLC-CHEMTAX analyses in the southern Baltic Sea, *Mar. Ecol.-Prog. Ser.*, 359, 69–87, doi:10.3354/meps07319, 2008.
- 20 Endo, H., Yoshimura, T., Kataoka, T., and Suzuki, K.: Effects of CO₂ and iron availability on phytoplankton and eubacterial community compositions in the northwest subarctic Pacific, *J. Exp. Mar. Biol. Ecol.*, 439, 160–175, doi:10.1016/j.jembe.2012.11.003, 2013.
- Engel, A., Zondervan, I., Aerts, K., Beaufort, L., Benthien, A., Chou, L., Delille, B., Gattuso, J.-P., Harlay, J., and Heemann, C.: Testing the direct effect of CO₂ concentration on a bloom of the coccolithophorid *Emiliania huxleyi* in mesocosm experiments, *Limnol. Oceanogr.*, 50, 493–507, doi:10.4319/lo.2005.50.2.0493, 2005.
- 25 Engel, A., Schulz, K. G., Riebesell, U., Bellerby, R., Delille, B., and Schartau, M.: Effects of CO₂ on particle size distribution and phytoplankton abundance during a mesocosm bloom experiment (PeECE II), *Biogeosciences*, 5, 509–521, doi:10.5194/bg-5-509-2008, 2008.
- 30 Engel, A., Piontek, J., Grossart, H.-P., Riebesell, U., Schulz, K. G., and Sperling, M.: Impact of CO₂ enrichment on organic matter dynamics during nutrient induced coastal phytoplankton blooms, *J. Plankton Res.*, 36, 641–657, doi:10.1093/plankt/fbt125, 2014.

Effect of elevated CO₂ on organic matter pools and fluxes in a summer

A. J. Paul et al.

Title Page

Abstract

Introduction

Conclusions

References

Tables

Figures



Back

Close

Full Screen / Esc

Printer-friendly Version

Interactive Discussion



Feistel, R., Weinreben, S., Wolf, H., Seitz, S., Spitzer, P., Adel, B., Nausch, G., Schneider, B., and Wright, D. G.: Density and Absolute Salinity of the Baltic Sea 2006–2009, *Ocean Sci.*, 6, 3–24, doi:10.5194/os-6-3-2010, 2010.

Feng, Y., Hare, C. E., Rose, J. M., Handy, S. M., DiTullio, G. R., Lee, P. A., Smith Jr., W. O., Pelouquin, J., Tozzi, S., Sun, J., Zhang, Y., Dunbar, R. B., Long, M. C., Sohst, B., Lohan, M., and Hutchins, D. A.: Interactive effects of iron, irradiance and CO₂ on Ross Sea phytoplankton, *Deep-Sea Res. Pt. I*, 57, 368–383, doi:10.1016/j.dsr.2009.10.013, 2010.

Fofonoff, N. P. and Millard Jr., R. C.: Algorithms for computation of fundamental properties of seawater, UNESCO Technical Papers in Marine Science, 44, 1–53, http://www.jodc.go.jp/info/ioc_doc/UNESCO_tech/059832eb.pdf, 1983.

Gasiūnaitė, Z. R., Cardoso, A. C., Heiskanen, A.-S., Henriksen, P., Kauppila, P., Olenina, I., Pilkaitytė, R., Purina, I., Razinkovas, A., Sagert, S., Schubert, H., and Wasmund, N.: Seasonality of coastal phytoplankton in the Baltic Sea: influence of salinity and eutrophication, *Estuar. Coast. Shelf. S.*, 65, 239–252, doi:10.1016/j.ecss.2005.05.018, 2005.

Gieskes, J. M.: Effect of temperature on pH of seawater, *Limnol. Oceanogr.*, 14, 679–685, 1969.

Grasshoff, K., Ehrhardt, M., Kremling, K., and Almgren, T.: *Methods of Seawater Analysis*, Verlag Chemie, Weinheim, 1983.

Hama, T., Kawashima, S., Shimotori, K., Satoh, Y., Omori, Y., Wada, S., Adachi, T., Hasegawa, S., Midorikawa, T., Ishii, M., Saito, S., Sasano, D., Endo, H., Nakayama, T., and Inouye, I.: Effect of ocean acidification on coastal phytoplankton composition and accompanying organic nitrogen production, *J. Oceanogr.*, 68, 183–194, doi:10.1007/s10872-011-0084-6, 2012.

Hansen, H. P. and Koroleff, F.: Determination of nutrients, in: *Methods of Seawater Analysis*, edited by: Grasshoff, K., Kremling, K., and Ehrhardt, M., Wiley Verlag Chemie GmbH, Weinheim, 159–228, 1983.

Hansen, H. P. and Koroleff, F.: Determination of nutrients, in: *Methods of Seawater Analysis*, edited by: Grasshoff, K., Kremling, K., and Ehrhardt, M., Wiley Verlag Chemie GmbH, Weinheim, Germany, 159–228, 1999.

Hare, C. E., Leblanc, K., DiTullio, G. R., Kudela, R. M., Zhang, Y., Lee, P. A., Riseman, S., and Hutchins, D. A.: Consequences of increased temperature and CO₂ for phytoplankton community structure in the Bering Sea, *Mar. Ecol.-Prog. Ser.*, 352, 9–16, 2007.

Effect of elevated CO₂ on organic matter pools and fluxes in a summer

A. J. Paul et al.

Title Page

Abstract

Introduction

Conclusions

References

Tables

Figures



Back

Close

Full Screen / Esc

Printer-friendly Version

Interactive Discussion



- Hein, M. and Sand-Jensen, K.: CO₂ increases oceanic primary production, *Nature*, 388, 526–527, doi:10.1038/41457, 1997.
- HELCOM: Climate Change in the Baltic Sea Area: HELCOM Thematic Assessment in 2013, Helsinki Commission, Helsinki, 2013.
- 5 Hoikkola, L.: Dynamics of Dissolved Organic Matter and its Bioavailability to Heterotrophic Bacteria in the Gulf of Finland, Northern Baltic Sea, University of Helsinki, Helsinki, 2012.
- Hopkins, F. E., Turner, S. M., Nightingale, P. D., Steinke, M., Bakker, D., and Liss, P. S.: Ocean acidification and marine trace gas emissions, *P. Natl. Acad. Sci. USA*, 107, 760–765, doi:10.1073/pnas.0907163107, 2010.
- 10 Hopkinson, B. M., Xu, Y., Shi, D., McGinn, P. J., and Morel, F. M. M.: The effect of CO₂ on the photosynthetic physiology of phytoplankton in the Gulf of Alaska, *Limnol. Oceanogr.*, 55, 2011–2024, doi:10.4319/lo.2010.55.5.2011, 2010.
- Hoppe, C. J. M., Hassler, C. S., Payne, C. D., Tortell, P. D., Rost, B., and Trimborn, S.: Iron limitation modulates ocean acidification effects on Southern Ocean phytoplankton communities, *PLoS ONE*, 8, e79890, doi:10.1371/journal.pone.0079890, 2013.
- 15 Joint, I., Doney, S., and Karl, D.: Will ocean acidification affect marine microbes?, *ISME J.*, 5, 1–7, doi:10.1038/ismej.2010.79, 2011.
- Jutterström, S., Andersson, H. C., Omstedt, A., and Malmaeus, J. M.: Multiple stressors threatening the future of the Baltic Sea–Kattegat marine ecosystem: implications for policy and management actions, *Mar. Pollut. Bull.*, 86, 468–480, doi:10.1016/j.marpolbul.2014.06.027, 2014.
- 20 Kahru, M., Håkansson, B., and Rud, O.: Distributions of the sea-surface temperature fronts in the Baltic Sea as derived from satellite imagery, *Cont. Shelf Res.*, 15, 663–679, doi:10.1016/0278-4343(94)E0030-P, 1995.
- 25 Kanoshina, I., Lips, U., and Leppänen, J.-M.: The influence of weather conditions (temperature and wind) on cyanobacterial bloom development in the Gulf of Finland (Baltic Sea), *Harmful Algae*, 2, 29–41, doi:10.1016/S1568-9883(02)00085-9, 2003.
- Kérouel, R. and Aminot, A.: Fluorometric determination of ammonia in sea and estuarine waters by direct segmented flow analysis, *Mar. Chem.*, 57, 265–275, doi:10.1016/S0304-4203(97)00040-6, 1997.
- 30 Kim, J.-M., Lee, K., Shin, K., Kang, J.-H., Lee, H.-W., Kim, M., Jang, P.-G., and Jang, M.-C.: The effect of seawater CO₂ concentration on growth of a natural phytoplankton assemblage in a controlled mesocosm experiment, *Limnol. Oceanogr.*, 51, 1629–1636, 2006.

Effect of elevated CO₂ on organic matter pools and fluxes in a summer

A. J. Paul et al.

Title Page

Abstract

Introduction

Conclusions

References

Tables

Figures



Back

Close

Full Screen / Esc

Printer-friendly Version

Interactive Discussion



Koeve, W. and Oschlies, A.: Potential impact of DOM accumulation on $f\text{CO}_2$ and carbonate ion computations in ocean acidification experiments, *Biogeosciences*, 9, 3787–3798, doi:10.5194/bg-9-3787-2012, 2012.

Law, C. S., Breitbarth, E., Hoffmann, L. J., McGraw, C. M., Langlois, R. J., LaRoche, J., Marriner, A., and Safi, K. A.: No stimulation of nitrogen fixation by non-filamentous diazotrophs under elevated CO₂ in the South Pacific, *Glob. Change Biol.*, 18, 3004–3014, doi:10.1111/j.1365-2486.2012.02777.x, 2012.

Lehmann, A. and Myrberg, K.: Upwelling in the Baltic Sea – a review, *J. Marine Syst.*, 74, S3–S12, doi:10.1016/j.jmarsys.2008.02.010, 2008.

Lips, I. and Lips, U.: Phytoplankton dynamics affected by the coastal upwelling events in the Gulf of Finland in July–August 2006, *J. Plankton Res.*, 32, 1269–1282, doi:10.1093/plankt/fbq049, 2010.

Lischka, S. et al.: *Biogeosciences*, in preparation, 2015.

Lomas, M. W., Hopkinson, B. M., Ryan, J. L. L. D. E., Shi, D. L., Xu, Y., and Morel, F. M. M.: Effect of ocean acidification on cyanobacteria in the subtropical North Atlantic, *Aquat. Microb. Ecol.*, 66, 211–222, doi:10.3354/ame01576, 2012.

Losh, J. L., Morel, F. M. M., and Hopkinson, B. M.: Modest increase in the C : N ratio of N-limited phytoplankton in the California Current in response to high CO₂, *Mar. Ecol.-Prog. Ser.*, 468, 31–42, doi:10.3354/meps09981, 2012.

Lueker, T. J., Dickson, A. G., and Keeling, C. D.: Ocean $p\text{CO}_2$ calculated from dissolved inorganic carbon, alkalinity, and equations for K₁ and K₂: validation based on laboratory measurements of CO₂ in gas and seawater at equilibrium, *Mar. Chem.*, 70, 105–119, doi:10.1016/S0304-4203(00)00022-0, 2000.

MacGilchrist, G. A., Shi, T., Tyrrell, T., Richier, S., Moore, C. M., Dumousseaud, C., and Achterberg, E. P.: Effect of enhanced $p\text{CO}_2$ levels on the production of dissolved organic carbon and transparent exopolymer particles in short-term bioassay experiments, *Biogeosciences*, 11, 3695–3706, doi:10.5194/bg-11-3695-2014, 2014.

Mackey, M. D., Mackey, D. J., Higgins, H. W., and Wright, S. W.: CHEMTAX – a program for estimating class abundances from chemical markers: application to HPLC measurements of phytoplankton, *Mar. Ecol.-Prog. Ser.*, 144, 265–283, doi:10.3354/meps144265, 1996.

Matthäus, W., Nausch, G., Lass, H. U., Nagel, K., and Siegel, H.: The Baltic Sea in 1998 – characteristic features of the current stagnation period, nutrient conditions in the surface layer

Effect of elevated CO₂ on organic matter pools and fluxes in a summer

A. J. Paul et al.

Title Page

Abstract

Introduction

Conclusions

References

Tables

Figures

⏪

⏩

◀

▶

Back

Close

Full Screen / Esc

Printer-friendly Version

Interactive Discussion



and exceptionally high deep water temperatures, *Deutsche Hydrographische Zeitschrift*, 51, 67–84, doi:10.1007/BF02763957, 1999.

Mehnert, G., Leunert, F., Cirés, S., Jöhnk, K. D., Rücker, J., Nixdorf, B., and Wiedner, C.: Competitiveness of invasive and native cyanobacteria from temperate freshwaters under various light and temperature conditions, *J. Plankton Res.*, 32, 1009–1021, doi:10.1093/plankt/fbq033, 2010.

Mehrbach, C., Culberson, C. H., Hawley, J. E., and Pytkowicz, R. M.: Measurement of apparent dissociation constants of carbonic acid in seawater at atmospheric pressure, *Limnol. Oceanogr.*, 18, 897–907, 1973.

Meier, H. E. M., Andersson, H. C., Eilola, K., Gustafsson, B. G., Kuznetsov, I., Müller-Karulis, B., Neumann, T., and Savchuk, O. P.: Hypoxia in future climates: a model ensemble study for the Baltic Sea, *Geophys. Res. Lett.*, 38, L24608, doi:10.1029/2011GL049929, 2011.

Mercado, J. M., Sobrino, C., Neale, P. J., Segovia, M., Reul, A., Amorim, A. L., Carrillo, P., Claquin, P., Cabrerizo, M. J., Leon, P., Lorenzo, M. R., Medina-Sanchez, J. M., Montecino, V., Napoleon, C., Prasil, O., Putzeys, S., Salles, S., and Yebra, L.: Effect of CO₂, nutrients and light on coastal plankton. II. Metabolic rates, *Aquat. Biol.*, 22, 43–57, doi:10.3354/ab00606, 2014.

Mosley, L. M., Husheer, S. L. G., and Hunter, K. A.: Spectrophotometric pH measurement in estuaries using thymol blue and m-cresol purple, *Mar. Chem.*, 91, 175–186, doi:10.1016/j.marchem.2004.06.008, 2004.

Nausch, M. et al.: *Biogeosciences*, in preparation, 2015.

Neale, P. J., Sobrino, C., Segovia, M., Mercado, J. M., Leon, P., Cortés, M. D., Tuite, P., Picazo, A., Salles, S., Cabrerizo, M. J., Prasil, O., Montecino, V., Reul, A., and Fuentes-Lema, A.: Effect of CO₂, nutrients and light on coastal plankton. I. Abiotic conditions and biological responses, *Aquat. Biol.*, 22, 25–41, doi:10.3354/ab00587, 2014.

Newbold, L. K., Oliver, A. E., Booth, T., Tiwari, B., DeSantis, T., Maguire, M., Andersen, G., Van der Gast, C. J., and Whiteley, A. S.: The response of marine picoplankton to ocean acidification, *Environ. Microbiol.*, 14, 2293–2307, doi:10.1111/j.1462-2920.2012.02762.x, 2012.

Nielsen, L. T., Jakobsen, H. H., and Hansen, P. J.: High resilience of two coastal plankton communities to twenty-first century seawater acidification: evidence from microcosm studies, *Mar. Biol. Res.*, 6, 542–555, doi:10.1080/17451000903476941, 2010.

Effect of elevated CO₂ on organic matter pools and fluxes in a summer

A. J. Paul et al.

Title Page

Abstract

Introduction

Conclusions

References

Tables

Figures



Back

Close

Full Screen / Esc

Printer-friendly Version

Interactive Discussion



- Nielsen, L. T., Hallegraeff, G. M., Wright, S. W., and Hansen, P. J.: Effects of experimental seawater acidification on an estuarine plankton community, *Aquat. Microb. Ecol.*, 65, 271–285, 2011.
- Nômmann, S., Sildam, J., Nôges, T., and Kahru, M.: Plankton distribution during a coastal upwelling event off Hiiumaa, Baltic Sea: impact of short-term flow field variability, *Cont. Shelf Res.*, 11, 95–108, doi:10.1016/0278-4343(91)90037-7, 1991.
- Paul, A. J. et al.: Biogeosciences, in preparation, 2015.
- Patey, M. D., Rijkenberg, M. J. A., Statham, P. J., Stinchcombe, M. C., Achterberg, E. P., and Mowlem, M.: Determination of nitrate and phosphate in seawater at nanomolar concentrations, *TrAC-Trend. Anal. Chem.*, 27, 169–182, doi:10.1016/j.trac.2007.12.006, 2008.
- Petersen, J. E., Dennison, W. C., Kennedy, V. S., and Kemp, W. M. (Eds.): *Enclosed Experimental Ecosystems and Scale: Tools for Understanding and Managing Coastal Ecosystems*, Springer Science & Business Media, New York, 2009.
- Pierrot, D. E., Wallace, D. W. R., and Lewis, E.: MS Excel Program Developed for CO₂ System Calculations, available at: http://cdiac.ornl.gov/ftp/co2sys/CO2SYS_calc_XLS_v2.1/ (last access: 21 October 2014), 2011.
- Redfield, A. C.: The biological control of chemical factors in the environment, *Am. Sci.*, 46, 205–221, 1958.
- Richardson, T. L. and Jackson, G. A.: Small phytoplankton and carbon export from the surface ocean, *Science*, 315, 838–840, doi:10.1126/science.1133471, 2007.
- Richier, S., Achterberg, E. P., Dumousseaud, C., Poulton, A. J., Suggett, D. J., Tyrrell, T., Zubkov, M. V., and Moore, C. M.: Phytoplankton responses and associated carbon cycling during shipboard carbonate chemistry manipulation experiments conducted around North-west European shelf seas, *Biogeosciences*, 11, 4733–4752, doi:10.5194/bg-11-4733-2014, 2014.
- Riebesell, U. and Tortell, P. D.: Effects of ocean acidification on pelagic organisms and ecosystems, in: *Ocean Acidification*, edited by: Gattuso, J.-P. and Hansson, L., Oxford University Press, Oxford, United Kingdom, 99, 2011.
- Riebesell, U., Schulz, K. G., Bellerby, R. G. J., Botros, M., Fritsche, P., Meyerhöfer, M., Neill, C., Nondal, G., Oschlies, A., Wohlers, J., and Zöllner, E.: Enhanced biological carbon consumption in a high CO₂ ocean, *Nature*, 450, 545–548, doi:10.1038/nature06267, 2007.
- Riebesell, U., Czerny, J., von Bröckel, K., Boxhammer, T., Büdenbender, J., Deckelnick, M., Fischer, M., Hoffmann, D., Krug, S. A., Lentz, U., Ludwig, A., Mucche, R., and Schulz, K. G.:

Effect of elevated CO₂ on organic matter pools and fluxes in a summer

A. J. Paul et al.

[Title Page](#)

[Abstract](#)

[Introduction](#)

[Conclusions](#)

[References](#)

[Tables](#)

[Figures](#)

[⏪](#)

[⏩](#)

[◀](#)

[▶](#)

[Back](#)

[Close](#)

[Full Screen / Esc](#)

[Printer-friendly Version](#)

[Interactive Discussion](#)



Technical Note: A mobile sea-going mesocosm system – new opportunities for ocean change research, *Biogeosciences*, 10, 1835–1847, doi:10.5194/bg-10-1835-2013, 2013.

Rossoll, D., Sommer, U., and Winder, M.: Community interactions dampen acidification effects in a coastal plankton system, *Mar. Ecol.-Prog. Ser.*, 486, 37–46, doi:10.3354/meps10352, 2013.

Rost, B., Zondervan, I., and Wolf-Gladrow, D.: Sensitivity of phytoplankton to future changes in ocean carbonate chemistry: current knowledge, contradictions and research directions, *Mar. Ecol.-Prog. Ser.*, 373, 227–237, doi:10.3354/meps07776, 2008.

Schernewski, G.: *Global Change and Baltic Coastal Zones*, Springer Science & Business Media, Dordrecht, 2011.

Schluter, L., Mohlenberg, F., Havskum, H., and Larsen, S.: The use of phytoplankton pigments for identifying and quantifying phytoplankton groups in coastal areas: testing the influence of light and nutrients on pigment/chlorophyll *a* ratios, *Mar. Ecol.-Prog. Ser.*, 192, 49–63, doi:10.3354/meps192049, 2000.

Schulz, K. G. and Riebesell, U.: Diurnal changes in seawater carbonate chemistry speciation at increasing atmospheric carbon dioxide, *Mar. Biol.*, 160, 1889–1899, doi:10.1007/s00227-012-1965-y, 2013.

Schulz, K. G., Riebesell, U., Bellerby, R. G. J., Biswas, H., Meyerhöfer, M., Müller, M. N., Egge, J. K., Nejtgaard, J. C., Neill, C., Wohlers, J., and Zöllner, E.: Build-up and decline of organic matter during PeECE III, *Biogeosciences*, 5, 707–718, doi:10.5194/bg-5-707-2008, 2008.

Schulz, K. G., Bellerby, R. G. J., Brussaard, C. P. D., Büdenbender, J., Czerny, J., Engel, A., Fischer, M., Koch-Klavnsen, S., Krug, S. A., Lischka, S., Ludwig, A., Meyerhöfer, M., Nondal, G., Silyakova, A., Stuhr, A., and Riebesell, U.: Temporal biomass dynamics of an Arctic plankton bloom in response to increasing levels of atmospheric carbon dioxide, *Biogeosciences*, 10, 161–180, doi:10.5194/bg-10-161-2013, 2013.

Schulz, K. G. et al.: in preparation, 2015.

Sharp, J.: Improved analysis for particulate organic carbon and nitrogen from seawater, *Limnol. Oceanogr.*, 19, 984–989, 1974.

Sommer, U., Stibor, H., Katechakis, A., Sommer, F., and Hansen, T.: Pelagic food web configurations at different levels of nutrient richness and their implications for the ratio fish production:primary production, *Hydrobiologia*, 484, 11–20, doi:10.1023/A:1021340601986, 2002.

Effect of elevated CO₂ on organic matter pools and fluxes in a summer

A. J. Paul et al.

Title Page

Abstract

Introduction

Conclusions

References

Tables

Figures

◀

▶

◀

▶

Back

Close

Full Screen / Esc

Printer-friendly Version

Interactive Discussion










- Vahtera, E., Conley, D. J., Gustafsson, B. G., Kuosa, H., Pitkänen, H., Savchuk, O. P., Tamminen, T., Viitasalo, M., Voss, M., Wasmund, N., and Wulff, F.: Internal ecosystem feedbacks enhance nitrogen-fixing cyanobacteria blooms and complicate management in the Baltic Sea, *AMBIO*, 36, 186–194, doi:10.1579/0044-7447(2007)36[186:IEFENC]2.0.CO;2, 2007.
- 5 Welschmeyer, N. A.: Fluorometric analysis of chlorophyll *a* in the presence of chlorophyll *b* and pheopigments, *Limnol. Oceanogr.*, 39, 1985–1992, doi:10.4319/lo.1994.39.8.1985, 1994.
- Wu, R. S. S.: Hypoxia: from molecular responses to ecosystem responses, *Mar. Pollut. Bull.*, 45, 35–45, doi:10.1016/S0025-326X(02)00061-9, 2002.
- Yoshimura, T., Nishioka, J., Suzuki, K., Hattori, H., Kiyosawa, H., and Watanabe, Y. W.: Impacts of elevated CO₂ on organic carbon dynamics in nutrient depleted Okhotsk Sea surface waters, *J. Exp. Mar. Biol. Ecol.*, 395, 191–198, doi:10.1016/j.jembe.2010.09.001, 2010.
- 10 Yoshimura, T., Suzuki, K., Kiyosawa, H., Ono, T., Hattori, H., Kuma, K., and Nishioka, J.: Impacts of elevated CO₂ on particulate and dissolved organic matter production: microcosm experiments using iron-deficient plankton communities in open subarctic waters, *J. Oceanogr.*, 69, 601–618, doi:10.1007/s10872-013-0196-2, 2013.
- Yoshimura, T., Sugie, K., Endo, H., Suzuki, K., Nishioka, J., and Ono, T.: Organic matter production response to CO₂ increase in open subarctic plankton communities: comparison of six microcosm experiments under iron-limited and -enriched bloom conditions, *Deep-Sea Res. Pt. I*, 94, 1–14, doi:10.1016/j.dsr.2014.08.004, 2014.
- 20 Zapata, M., Rodriguez, F., and Garrido, J. L.: Separation of chlorophylls and carotenoids from marine phytoplankton: a new HPLC method using a reversed phase C-8 column and pyridine-containing mobile phases, *Mar. Ecol.-Prog. Ser.*, 195, 29–45, doi:10.3354/meps195029, 2000.
- Zhang, J.-Z. and Chi, J.: Automated analysis of nanomolar concentrations of phosphate in natural waters with liquid waveguide, *Environ. Sci. Technol.*, 36, 1048–1053, doi:10.1021/es011094v, 2002.
- 25

Effect of elevated CO₂ on organic matter pools and fluxes in a summer

A. J. Paul et al.

Table 2. Volumes of CO₂-enriched seawater added for the CO₂ manipulation indicating day of addition and total manipulation volumes. Symbols and colours indicated here indicated here are used in all following figures.

Mesocosm	M1	M5	M7	M6	M3	M8	Baltic	
Target $f\text{CO}_2$ (μatm)	ambient/ control	ambient/ control	600	950	1300	1650	ambient	
Average $f\text{CO}_2$ (μatm) $t1 - t43$	365	368	497	821	1007	1231	417	
Average $f\text{CO}_2$ (μatm) $t1 - t30$	346	348	494	868	1075	1333	343	
Symbol								
Day	$t0$	–	–	20 L	50 L	65 L	75 L	–
	$t1$	–	–	10 L	40 L	50 L	65 L	–
	$t2$	–	–	10 L	30 L	45 L	50 L	–
	$t3$	–	–	5 L	8 L	9 L	10 L	–
	$t15$	–	–	–	9 L	12 L	18 L	–
	Total	–	–	45 L	137 L	181 L	218 L	–

Title Page

Abstract

Introduction

Conclusions

References

Tables

Figures



Back

Close

Full Screen / Esc

Printer-friendly Version

Interactive Discussion



Effect of elevated CO₂ on organic matter pools and fluxes in a summer

A. J. Paul et al.

Title Page

Abstract

Introduction

Conclusions

References

Tables

Figures

⏪

⏩

◀

▶

Back

Close

Full Screen / Esc

Printer-friendly Version

Interactive Discussion



Table 3. Summary of linear regression analyses of CO₂ effects on particulate and dissolved matter and sediment trap material including elemental stoichiometry in different size fractions for each experimental phase. f CO₂ and the parameter were averaged for each phase and using a linear model, a regression analysis was done to test for statistical significance of a potential CO₂ effect. Significant positive effects detected are in bold, significant negative effects of CO₂ are in italics. Degrees of freedom = 4.

	Parameter	Particulate matter			Dissolved matter and Chl <i>a</i>			Sediment material					
		ρ	Multiple R^2	<i>F</i> statistic	Parameter	ρ	Multiple R^2	<i>F</i> statistic	Parameter	ρ	Multiple R^2	<i>F</i> statistic	
Phase I	TPC	total	0.152	0.438	3.113	Nitrate (0–17 m)	0.547	0.098	0.433	Total accumulated material	0.265	0.296	1.680
Phase II			0.902	0.761	12.760		0.602	0.074	0.320		0.593	0.078	0.336
Phase III			0.011	0.834	20.070		0.768	0.034	0.105		0.945	0.001	0.005
Phase I	TPC < 55 μ m		0.580	0.083	0.363	Nitrate (0–10 m)	0.709	0.085	0.185	Total accumulated material in phase	0.265	0.296	1.680
Phase II			0.536	0.103	0.458		0.033	<i>0.718</i>	<i>10.170</i>		0.799	0.018	0.074
Phase III			0.759	0.026	0.108		0.540	0.101	0.448		0.372	0.202	1.010
Phase I	TPC < 10 μ m	–	–	–	DIP (0–17 m)	0.486	0.128	0.589	Cumulative TPC	0.752	0.028	0.115	
Phase II			0.036	0.929	26.120		0.076	0.587	5.679		0.902	0.004	0.017
Phase III		in phase	0.187	0.661	3.899		<i>0.003</i>	<i>0.910</i>	<i>40.170</i>		0.386	0.191	0.947
Phase I	PON total		0.668	0.051	0.214	DIP (0–10 m)	0.651	0.056	0.239	Cumulative PON in phase	0.848	0.010	0.042
Phase II			0.490	0.126	0.576		0.075	0.589	5.737		0.662	0.052	0.222
Phase III			0.001	0.940	62.890		<i>0.030</i>	<i>0.732</i>	<i>10.950</i>		0.309	0.253	1.357
Phase I	PON < 55 μ m		0.640	0.060	0.255	NH ₄ ⁺ (0–17 m)	0.225	0.340	2.058	Cumulative TPP in phase	0.621	0.067	0.286
Phase II			0.516	0.113	0.508		0.297	0.265	1.439		0.749	0.028	0.117
Phase III			0.381	0.195	0.968		0.217	0.349	2.147		0.358	0.212	1.079
Phase I	PON < 10 μ m	–	–	–	Dissolved silicate	0.389	0.189	0.930	Cumulative BSi in phase	0.950	0.001	0.005	
Phase II			0.207	0.630	3.401		0.272	0.288	1.617		0.850	0.010	0.041
Phase III			0.098	0.813	8.703		0.642	0.059	0.252		0.108	0.515	4.255
Phase I	TPP		0.084	0.567	5.240	P*	0.554	0.094	0.416				
Phase II			0.363	0.208	1.050		0.549	0.096	0.427				
Phase III			0.004	0.897	34.690		<i>0.003</i>	<i>0.918</i>	<i>44.470</i>				
Phase I	Biogenic silica (BSi)		0.070	0.601	6.032	DOC	0.324	0.240	1.262				
Phase II			0.034	0.717	10.120		0.230	0.334	2.006				
Phase III			0.553	0.095	0.419		0.005	0.882	29.920				
Phase I	C : N in total POM		0.653	0.056	0.236	DON	0.652	0.056	0.236				
Phase II			0.020	0.779	14.080		0.358	0.212	1.079				
Phase III			0.050	0.659	7.716		0.926	0.002	0.010				
Phase I	C : N in POM < 55 μ m		0.487	0.128	0.587	DOP	0.914	0.003	0.013				
Phase II			0.208	0.360	2.249		0.391	0.188	0.924				
Phase III			0.037	0.704	9.516		0.812	0.016	0.065				
Phase I	C : N in POM < 10 μ m	–	–	–	Chl <i>a</i> (0–17 m)	0.796	0.019	0.076					
Phase II			0.009	0.982	105.800		0.020	0.780	14.180				
Phase III			0.164	0.699	4.643		0.022	0.766	13.070				
Phase I	N : P in total POM		0.707	0.039	0.163	Chl <i>a</i> (0–10 m)	0.227	0.337	2.037				
Phase II			0.848	0.010	0.042		0.034	0.714	9.995				
Phase III			0.397	0.184	0.900		0.008	0.859	24.320				
Phase I	C : P in total POM		0.507	0.117	0.529								
Phase II			0.582	0.082	0.358								
Phase III			0.056	0.641	7.133								
Phase I	C : BSi in total POM		0.989	0.000	0.000								
Phase II			0.127	0.480	3.695								
Phase III			0.307	0.255	1.370								

Effect of elevated CO₂ on organic matter pools and fluxes in a summer

A. J. Paul et al.

Title Page

Abstract

Introduction

Conclusions

References

Tables

Figures

⏪

⏩

◀

▶

Back

Close

Full Screen / Esc

Printer-friendly Version

Interactive Discussion



Table 4. Results of linear regression analyses of CO₂ and percentage contribution of phytoplankton groups to chlorophyll *a*.

Phytoplankton group	Phase I			Phase II			Phase III		
	<i>p</i>	Multiple <i>R</i> ²	<i>F</i> statistic	<i>p</i>	Multiple <i>R</i> ²	<i>F</i> statistic	<i>p</i>	Multiple <i>R</i> ²	<i>F</i> statistic
Prasinophytes	0.645	0.058	0.248	0.095	0.543	4.751	0.025	0.754	12.270
Cryptophytes	0.995	0.001	0.004	0.463	0.141	0.657	<i>0.041</i>	<i>0.687</i>	<i>8.789</i>
Chlorophytes	0.631	0.063	0.269	0.244	0.317	1.860	0.008	0.857	24.020
Cyanobacteria	0.224	0.341	2.067	0.421	0.167	0.803	0.153	0.4374	3.110
Diatoms	0.866	0.008	0.324	0.515	0.113	0.508	<i>0.009</i>	<i>0.8494</i>	<i>22.560</i>
Euglenophytes	0.962	0.001	0.003	0.438	0.156	0.741	0.976	0.000	0.001

Effect of elevated CO₂ on organic matter pools and fluxes in a summer

A. J. Paul et al.

[Title Page](#)
[Abstract](#)
[Introduction](#)
[Conclusions](#)
[References](#)
[Tables](#)
[Figures](#)
[Back](#)
[Close](#)
[Full Screen / Esc](#)
[Printer-friendly Version](#)
[Interactive Discussion](#)

Table 5. Summary of linear regression analyses done on absolute concentrations of phytoplankton pigments for the three experiment phases in different size fractions. Bold indicated significant positive effect and italics indicates significant negative effect of CO₂ concentration. ND indicates pigment was not detected. Where no pigment was detected in any phase in any size fraction, results were not included in this table.

Pigment	Size fraction	Phase I			Phase II			Phase III		
		<i>p</i>	Multiple <i>R</i> ²	<i>F</i> statistic	<i>p</i>	Multiple <i>R</i> ²	<i>F</i> statistic	<i>p</i>	Multiple <i>R</i> ²	<i>F</i> statistic
Chlorophyll <i>a</i>	total	0.470	0.137	0.636	0.008	0.854	23.440	0.081	0.573	5.377
	< 2 μm	0.014	0.815	17.650	0.658	0.053	0.228	0.659	0.057	0.227
	> 20 μm	0.009	0.850	22.720	0.011	0.836	20.440	0.273	0.288	1.616
Chlorophyll <i>b</i>	total	0.143	0.454	3.321	0.034	0.713	9.920	0.885	0.006	0.024
	< 2 μm	0.815	0.015	0.063	0.726	0.034	0.141	0.369	0.204	1.025
	> 20 μm	0.001	0.944	66.940	0.004	0.896	34.320	ND	ND	ND
Chlorophyll C2	total	0.283	0.278	1.538	<i>0.026</i>	<i>0.750</i>	<i>12.010</i>	0.371	0.202	1.015
	< 2 μm	0.877	0.007	0.027	0.437	0.157	0.745	0.876	0.007	0.028
	> 20 μm	ND	ND	ND	0.094	0.544	4.765	ND	ND	ND
Canthaxanthin	total	0.031	0.726	10.590	ND	ND	ND	ND	ND	ND
	< 2 μm	0.078	0.582	5.576	ND	ND	ND	0.973	ND	0.001
	> 20 μm	ND	ND	ND	ND	ND	ND	ND	ND	ND
Fucoxanthin	total	0.876	0.007	0.028	0.420	0.168	0.807	0.371	0.202	1.012
	< 2 μm	0.131	0.472	3.581	0.374	0.200	1.000	0.257	0.304	1.743
	> 20 μm	0.649	0.057	0.242	0.370	0.201	1.020	0.037	0.705	9.560
Myxoxanthophyll	total	0.056	0.642	7.157	0.755	0.027	0.112	ND	ND	ND
	< 2 μm	ND	ND	ND	ND	ND	ND	ND	ND	ND
	> 20 μm	ND	ND	ND	ND	ND	ND	ND	ND	ND
Neoxanthin	total	0.940	0.002	0.007	0.006	0.880	29.310	0.089	0.555	4.986
	< 2 μm	0.030	0.730	10.820	0.66	0.053	0.225	0.820	0.015	0.059
	> 20 μm	0.005	0.890	32.470	0.003	0.907	39.090	ND	ND	ND
Prasinanthin	total	0.040	0.691	8.947	0.001	0.945	68.540	ND	ND	ND
	< 2 μm	0.517	0.112	0.504	0.072	0.595	5.883	0.503	0.119	0.539
	> 20 μm	0.001	0.951	77.440	0.003	0.917	44.360	ND	ND	ND
Violaxanthin	total	0.030	0.731	10.840	0.002	0.929	52.580	0.035	0.711	9.839
	< 2 μm	0.017	0.797	15.710	0.854	0.010	0.038	0.882	0.006	0.025
	> 20 μm	0.002	0.926	49.770	0.002	0.925	49.480	0.982	ND	0.001

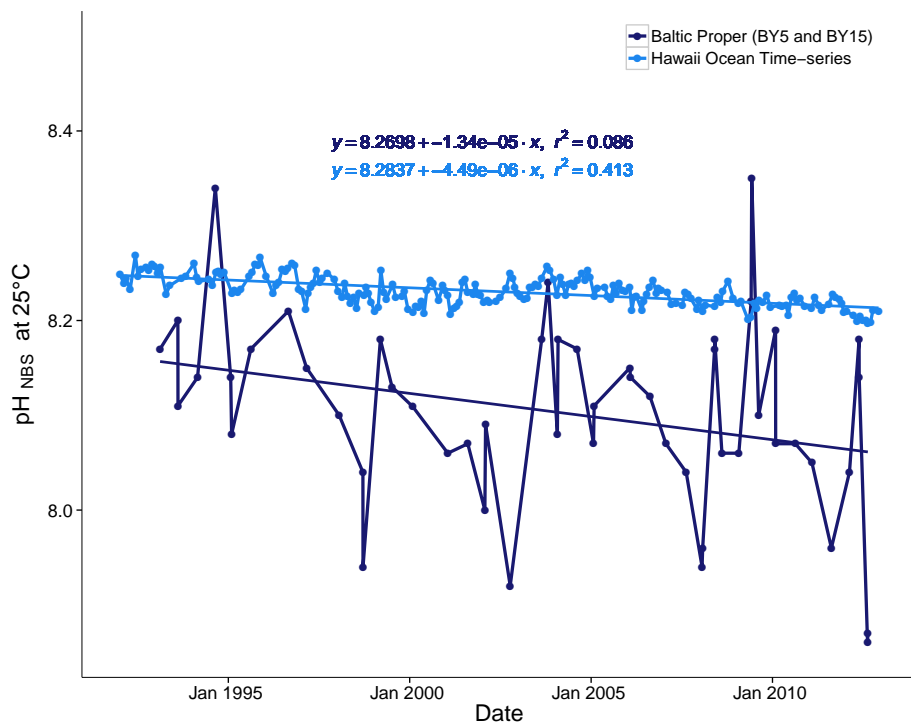


Figure 1. Time series of pH_{NBS} (25°C) from measurements from the Baltic Sea (The International Council for the Exploration of the Sea, 2014) and from calculations using DIC and TA the HOT data set (Dore et al., 2009) and CO_2SYS (Pierrot et al., 2011) indicating pH decrease between 1992 and 2012. Baltic Sea data set shows higher seasonal and interannual variation than North Tropical Pacific due to larger temperature and biomass fluctuations.

Effect of elevated CO_2 on organic matter pools and fluxes in a summer

A. J. Paul et al.

Title Page	
Abstract	Introduction
Conclusions	References
Tables	Figures
◀	▶
◀	▶
Back	Close
Full Screen / Esc	
Printer-friendly Version	
Interactive Discussion	



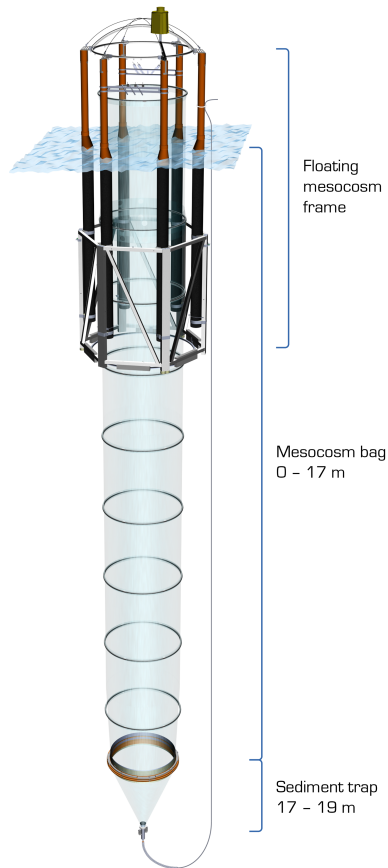


Figure 2. Diagram of Kiel Off-Shore Mesocosm for future Ocean Simulations showing floating frame, mesocosm bag and attached sediment trap. Source: GEOMAR.

Effect of elevated CO₂ on organic matter pools and fluxes in a summer

A. J. Paul et al.

Title Page

Abstract

Introduction

Conclusions

References

Tables

Figures

◀

▶

◀

▶

Back

Close

Full Screen / Esc

Printer-friendly Version

Interactive Discussion



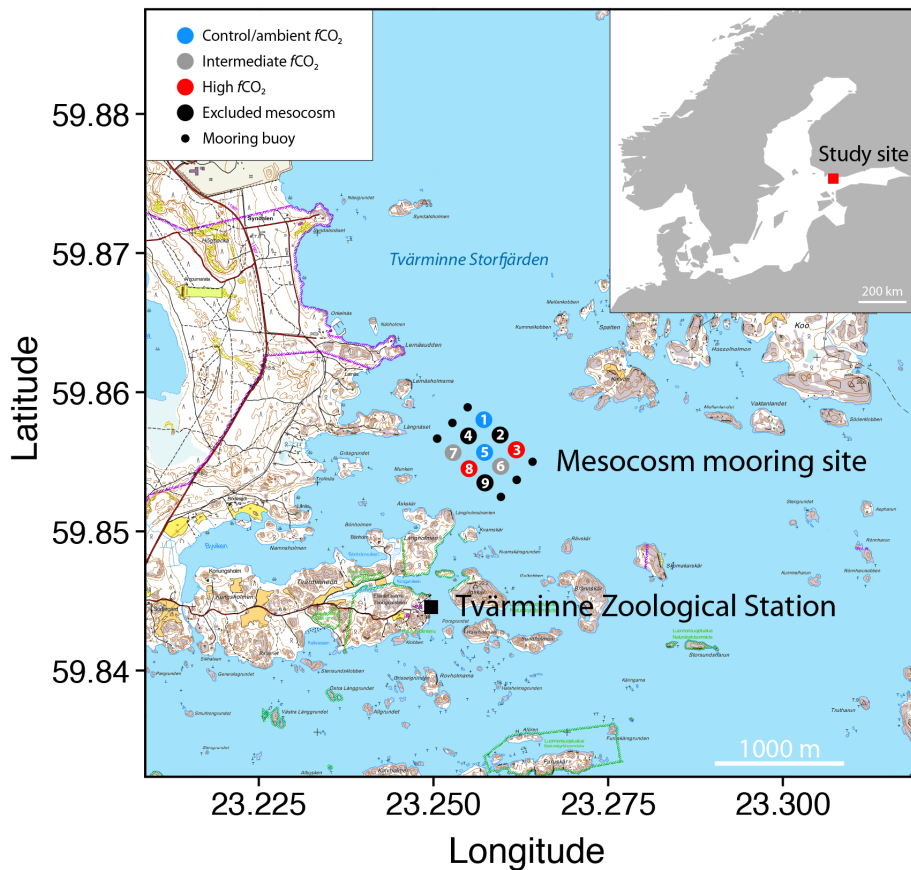


Figure 3. Map of study area (inset) and mesocosm mooring site in the Tvärminne Storöfjärden, off the Hanko Peninsula close to the entrance to the Gulf of Finland in the Baltic Sea. Mesocosm representation is not to scale. Map contains data from the National Land Survey of Finland Topographic Database, accessed March 2015.

Effect of elevated CO_2 on organic matter pools and fluxes in a summer

A. J. Paul et al.

Title Page	
Abstract	Introduction
Conclusions	References
Tables	Figures
◀	▶
◀	▶
Back	Close
Full Screen / Esc	
Printer-friendly Version	
Interactive Discussion	



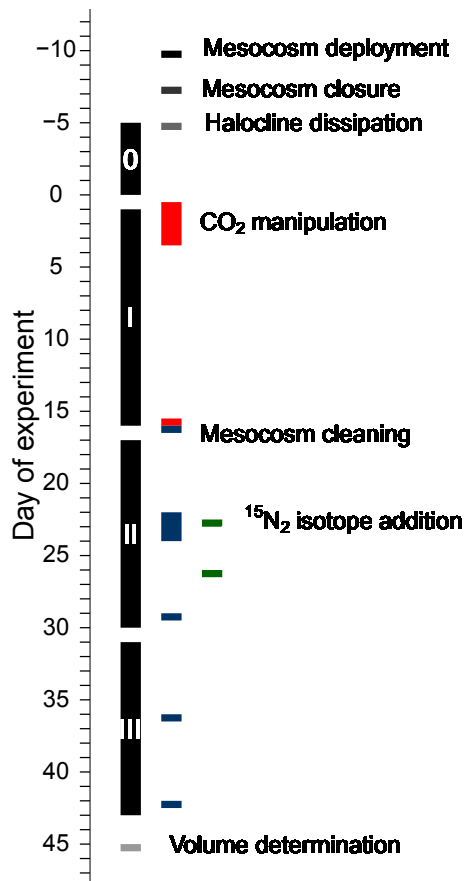


Figure 4. Experiment timeline indicating important activities such as CO₂ manipulations (red), cleaning (dark blue), phases (black labelled with 0, I, II and III for Phases 0, I, II and III respectively), volume determination (light grey) and isotope addition (dark green). Distinction of experimental phases is described in Sect. 3.1.

Effect of elevated CO₂ on organic matter pools and fluxes in a summer

A. J. Paul et al.

Title Page

Abstract Introduction

Conclusions References

Tables Figures

◀ ▶

◀ ▶

Back Close

Full Screen / Esc

Printer-friendly Version

Interactive Discussion



Effect of elevated CO₂ on organic matter pools and fluxes in a summer

A. J. Paul et al.

Title Page

Abstract

Introduction

Conclusions

References

Tables

Figures

◀

▶

◀

▶

Back

Close

Full Screen / Esc

Printer-friendly Version

Interactive Discussion

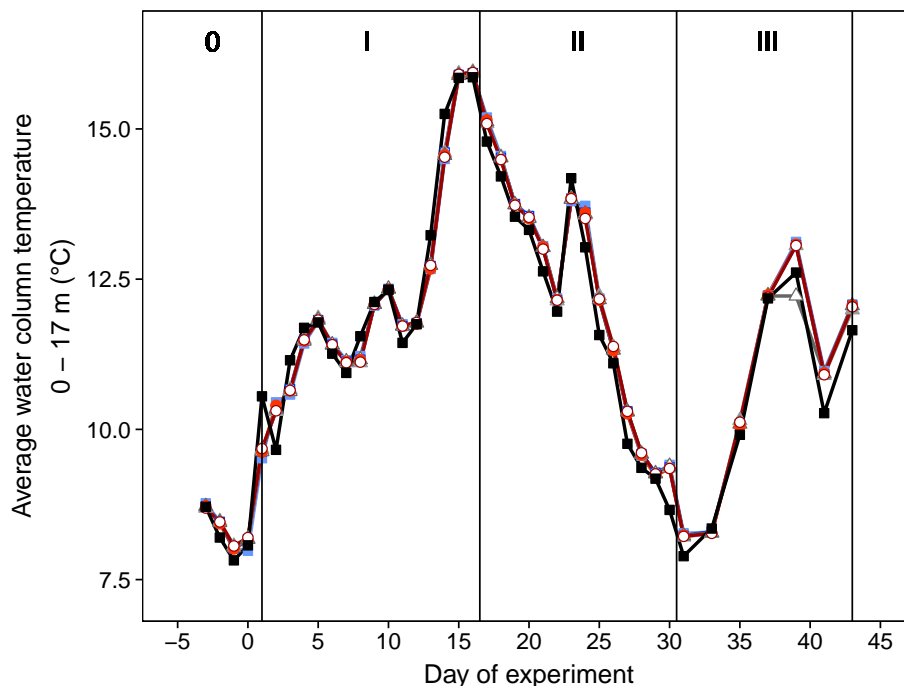


Figure 5. Variation in average water column temperature for all mesocosms and surrounding water during the study period. CO₂ enrichment (after t_0) and temperature variations defined experimental phases. Phase 0 = no CO₂ treatments, Phase 1 = warming, Phase II = cooling, Phase III = 2nd warming phase until end of the experiment at t_{43} . Colours and symbols are described in Table 2.

Effect of elevated CO₂ on organic matter pools and fluxes in a summer

A. J. Paul et al.

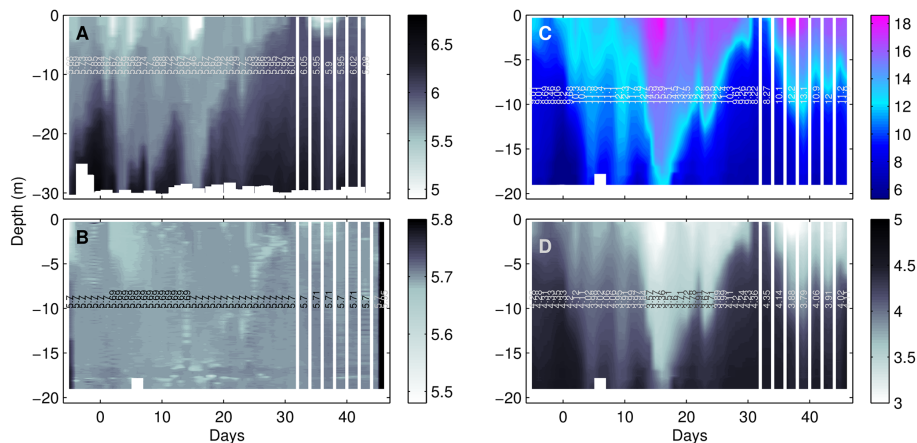


Figure 6. CTD profiles taken between t_5 and t_{46} for (a) salinity of surrounding water (Baltic), and (b) salinity, (c) temperature ($^{\circ}\text{C}$), and (d) density of M8 (σ_T in kg m^{-3}). M8 profiles are representative for all mesocosms. White vertical lines indicate CTD profiles were taken every second day after t_{31} .

Title Page

Abstract

Introduction

Conclusions

References

Tables

Figures

◀

▶

◀

▶

Back

Close

Full Screen / Esc

Printer-friendly Version

Interactive Discussion



Effect of elevated CO₂ on organic matter pools and fluxes in a summer

A. J. Paul et al.

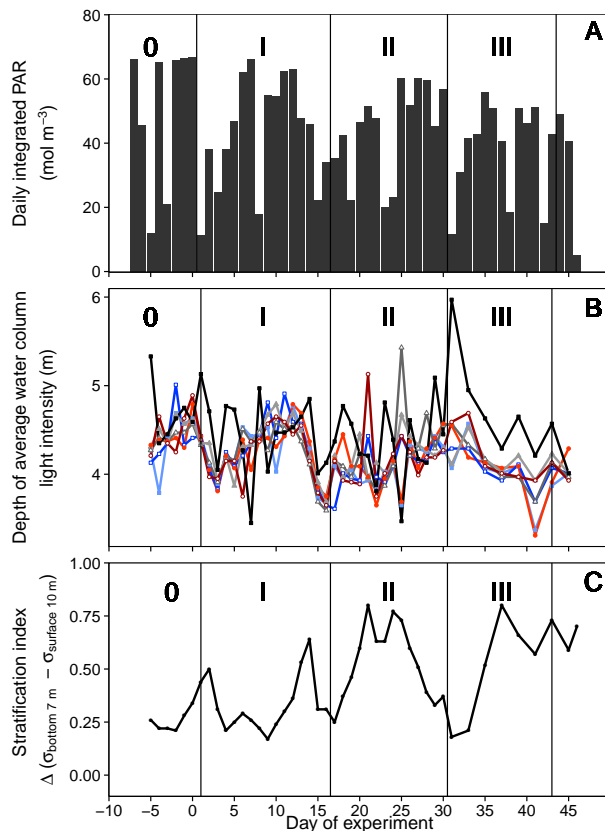


Figure 7. (a) Daily integrated incoming photosynthetically active radiation (PAR) measured by a unobstructed sensor on land during the study period, (b) depth of average water column light intensity calculated from CTD PAR sensor profiles between 0 and 17 m deep, (c) stratification index calculated from σ_T difference between the top 10 m and bottom 7 m in M8 as representative for all mesocosms. Symbols and colours for 7B are described in Table 2.

Title Page

Abstract

Introduction

Conclusions

References

Tables

Figures

◀

▶

◀

▶

Back

Close

Full Screen / Esc

Printer-friendly Version

Interactive Discussion



Effect of elevated CO₂ on organic matter pools and fluxes in a summer

A. J. Paul et al.

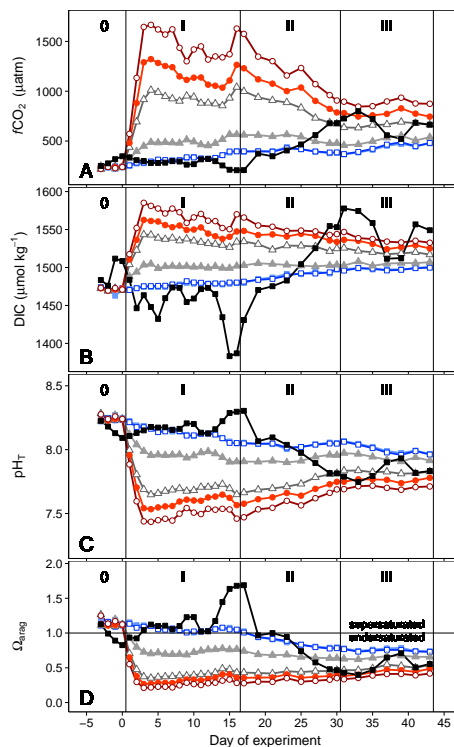


Figure 8. Dynamics in carbonate chemistry speciation with (a) calculated fugacity of CO₂, (b) measured dissolved inorganic carbon concentrations, (c) measured pH on total scale and calculated for in-situ temperatures, (d) calculated saturation state (Ω) of calcium carbonate (aragonite). Ω_{arag} and $f\text{CO}_2$ were calculated from DIC and TA using the stoichiometric equilibrium constants for carbonic acid of Mehrbach et al. (1973) as refitted by Lueker et al. (2000). Colours and symbols are described in Table 2.

Effect of elevated CO₂ on organic matter pools and fluxes in a summer

A. J. Paul et al.

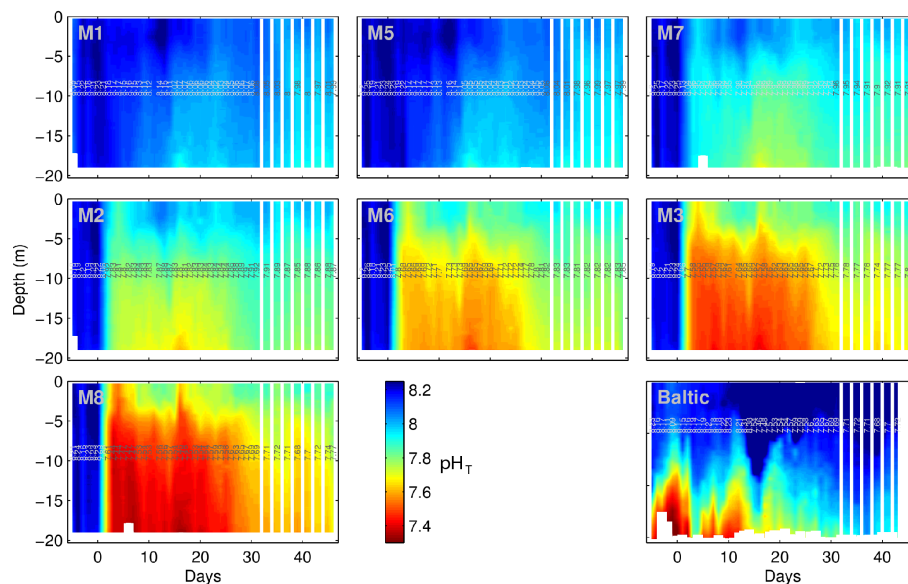
[Title Page](#)[Abstract](#)[Introduction](#)[Conclusions](#)[References](#)[Tables](#)[Figures](#)[Back](#)[Close](#)[Full Screen / Esc](#)[Printer-friendly Version](#)[Interactive Discussion](#)

Figure 9. Vertical pH_T profiles taken using a pH sensor on a hand-operated CTD during the experiment in the mesocosms and in the surrounding water, here named “Baltic”. For details of CTD operations and pH_T calculations, see Sect. 2.5.1. White vertical lines indicate CTD profiles were taken every second day after *t31*.

Effect of elevated CO₂ on organic matter pools and fluxes in a summer

A. J. Paul et al.

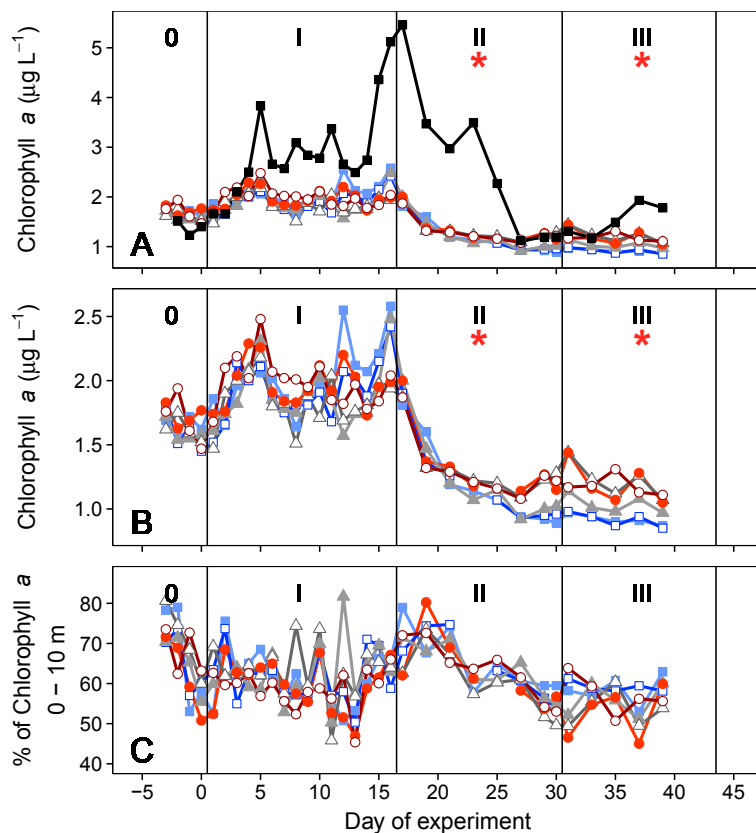


Figure 10. Temporal dynamics in (a) chlorophyll *a* (0–17 m) including surrounding water and (b) mesocosms only, and (c) percent of total chlorophyll *a* in the upper 10 m. Colours and symbols are described in Table 2. Red asterisk denotes significant positive effect of CO₂ (* = $p < 0.05$).

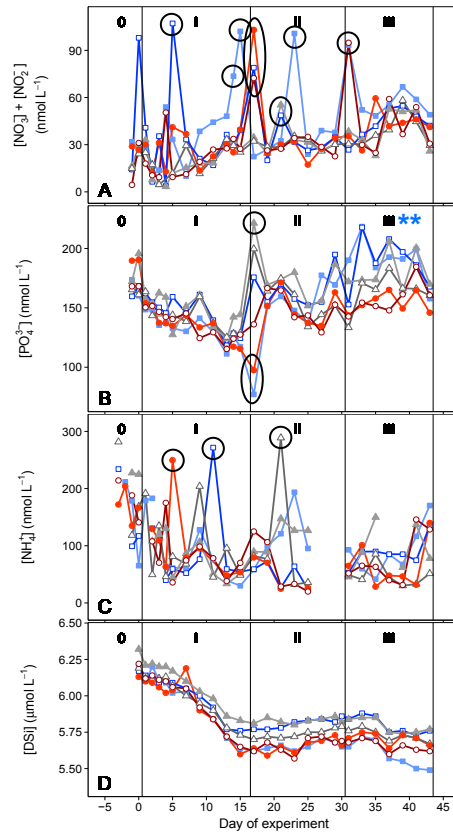


Figure 11. Temporal variation in concentrations of **(a)** dissolved nitrate + nitrite, **(b)** dissolved inorganic phosphate, **(c)** ammonium, **(d)** dissolved silicate. Colours and symbols are described in Table 2. Blue asterisk denotes a statistically significant negative effect of CO₂ (** = $p < 0.01$). Outliers (Grubb's test; see methods) are indicated by black circles and were excluded from linear regression analyses.

Effect of elevated CO₂ on organic matter pools and fluxes in a summer

A. J. Paul et al.

Title Page

Abstract Introduction

Conclusions References

Tables Figures

◀ ▶

◀ ▶

Back Close

Full Screen / Esc

Printer-friendly Version

Interactive Discussion



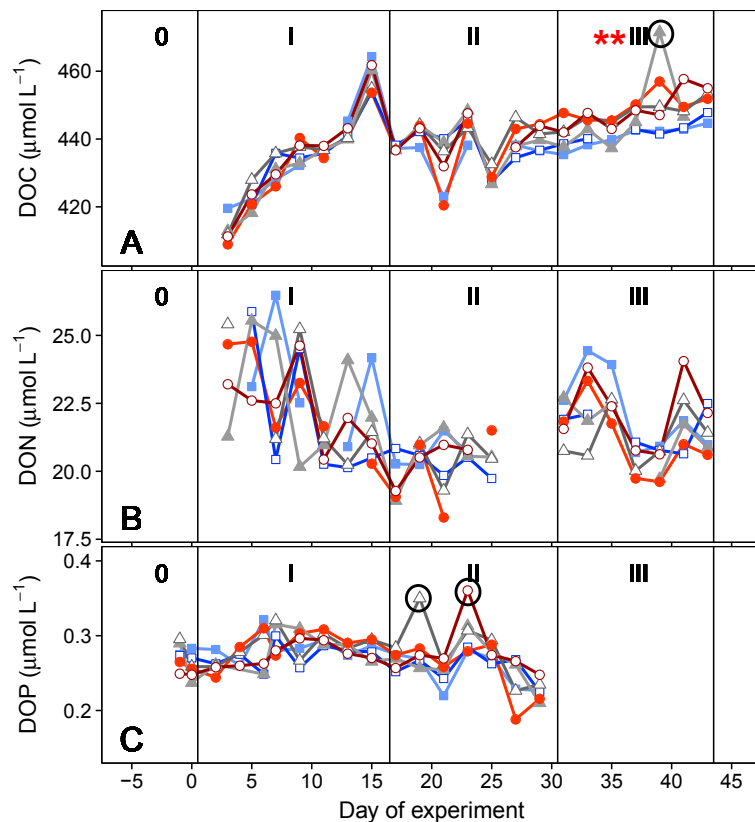


Figure 12. Temporal variation in concentrations of (a) dissolved organic carbon, (b) dissolved organic nitrogen, (c) dissolved organic phosphorus. CO₂ treatments are indicated by colours and symbols described in Table 2. Red asterisks denotes a statistically significant positive effect of CO₂ (** = $p < 0.01$). Outliers (Grubb's test; see methods) are indicated by black circles and were excluded from linear regression analyses.

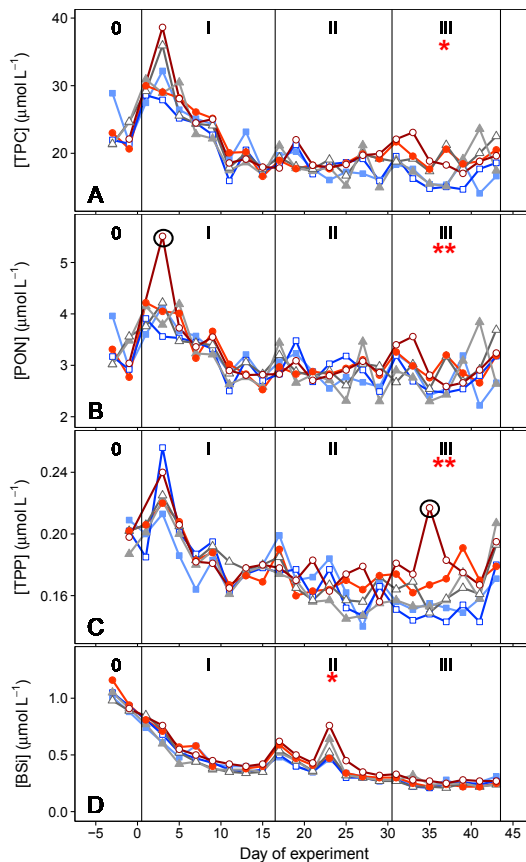


Figure 13. Temporal dynamics in concentrations of **(a)** total particulate carbon, **(b)** total particulate organic nitrogen, **(c)** total particulate phosphorus, and **(d)** particulate biogenic silica. Colours and symbols are described in Table 2. Red asterisk denotes significant positive effect of CO₂ (* = $p < 0.05$, ** = $p < 0.01$). Outliers (Grubb's test; see methods) are indicated by black circles and were excluded from linear regression analyses.

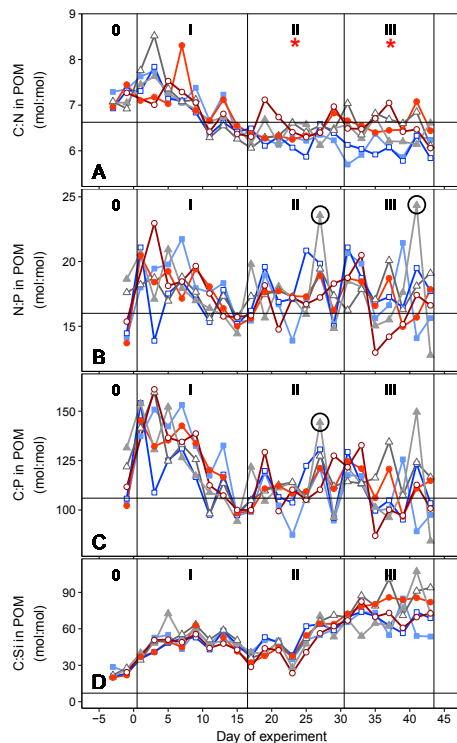


Figure 14. Temporal dynamics of elemental stoichiometry in particulate organic matter: **(a)** carbon to nitrogen, **(b)** nitrogen to phosphorus, **(c)** carbon to phosphorus, **(d)** carbon to biogenic silica. Horizontal lines indicate Redfield stoichiometry (C : N : P : Si = 106 : 16 : 1 : 15; Redfield, 1958). Colours and symbols for different treatments are described in Table 2. Red asterisk denotes significant positive effect of CO₂ (* = $p < 0.05$). Outliers (Grubb's test; see methods) are indicated by black circles and were excluded from linear regression analyses.

Effect of elevated CO₂ on organic matter pools and fluxes in a summer

A. J. Paul et al.

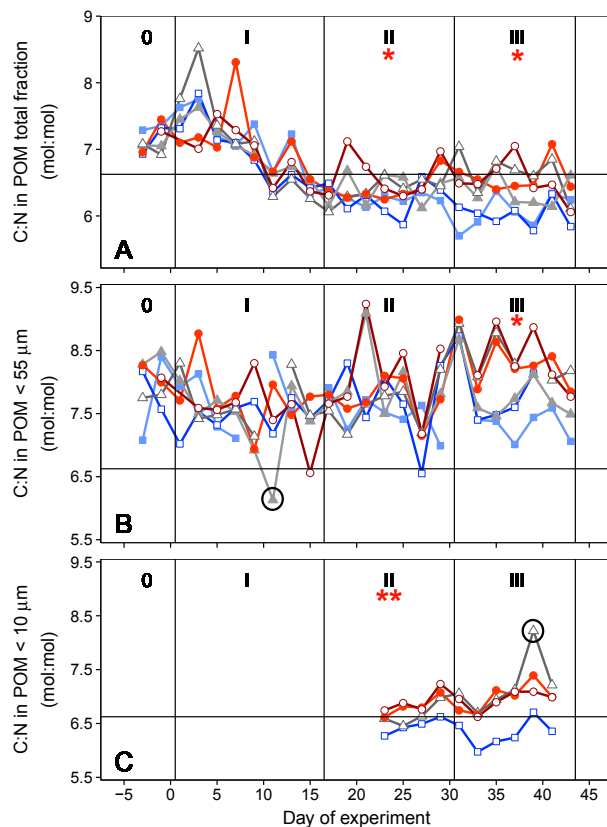


Figure 15. Elemental stoichiometry of C:N in suspended particulate matter for different size fractions during the study period, where (a) shows total fraction, (b) < 55 μm, and (c) < 10 μm. Colours and symbols for each CO₂ treatment are described in Table 2. Red asterisk denotes significant positive effect of CO₂ (* = $p < 0.05$, ** = $p < 0.01$). Outliers (Grubb's test; see methods) are indicated by black circles and were excluded from linear regression analyses.

Effect of elevated CO₂ on organic matter pools and fluxes in a summer

A. J. Paul et al.

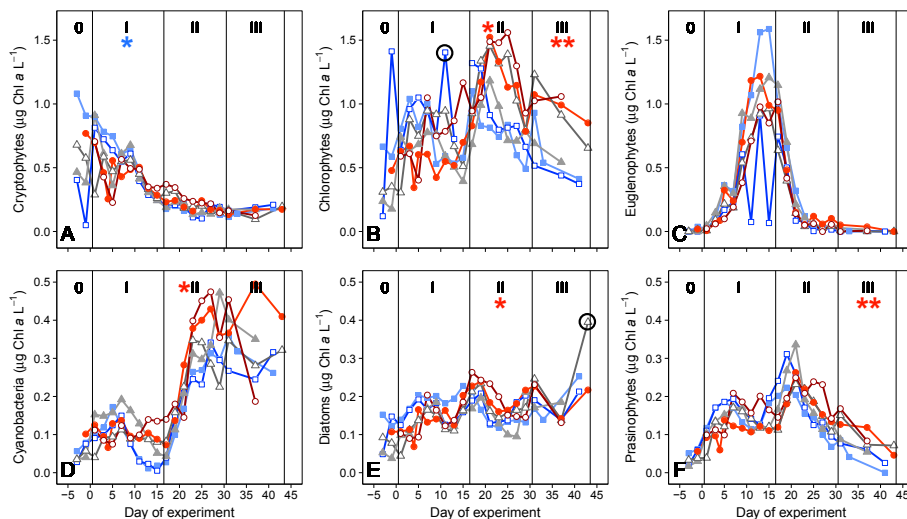


Figure 16. Contribution to total chlorophyll *a* by different phytoplankton groups as calculated by CHEMTAX from HPLC pigment analyses: (a) cryptophytes, (b) chlorophytes, (c) cyanobacteria, (d) euglenophytes, (e) diatoms, and (f) prasinophytes. Colours and symbols for each CO₂ treatment are described in Table 2. Red asterisk denotes significant positive effect and blue asterisk a significant negative effect of CO₂ (* = $p < 0.05$, ** = $p < 0.01$). Outliers are indicated by black circles and were excluded from linear regression analyses.

Title Page

Abstract

Introduction

Conclusions

References

Tables

Figures

◀

▶

◀

▶

Back

Close

Full Screen / Esc

Printer-friendly Version

Interactive Discussion



Effect of elevated CO₂ on organic matter pools and fluxes in a summer

A. J. Paul et al.

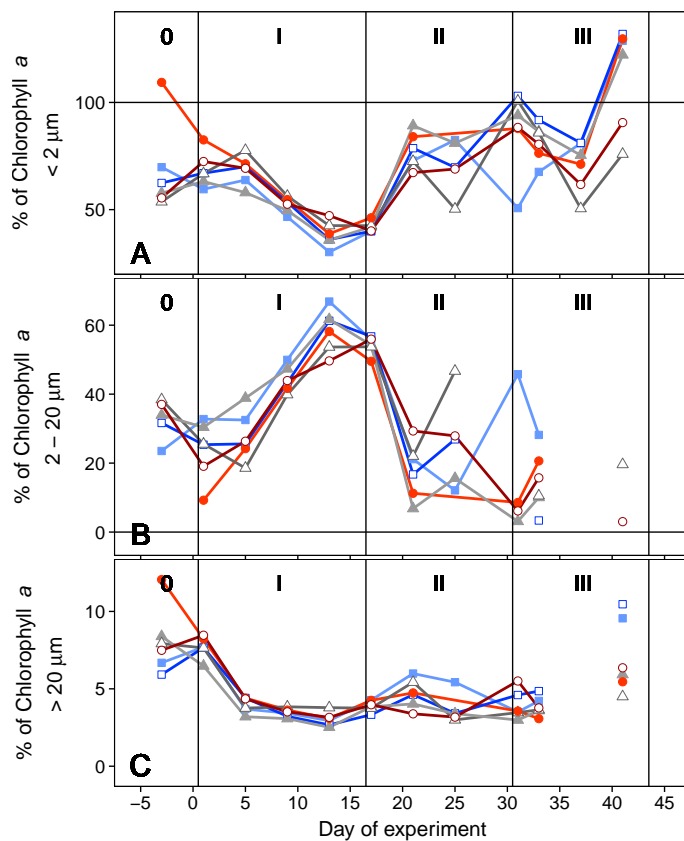


Figure 17. Relative contribution of different size fractions to total chlorophyll *a*. Size fraction 2–20 μm was calculated as a mass balance from total fraction and the two size fractions $< 2 \mu\text{m}$ and $> 20 \mu\text{m}$. Colours and symbols for different treatments are described in Table 2. Values larger than 100% or smaller than 0% are due to errors in mass balance calculation.

Title Page

Abstract

Introduction

Conclusions

References

Tables

Figures

◀

▶

◀

▶

Back

Close

Full Screen / Esc

Printer-friendly Version

Interactive Discussion



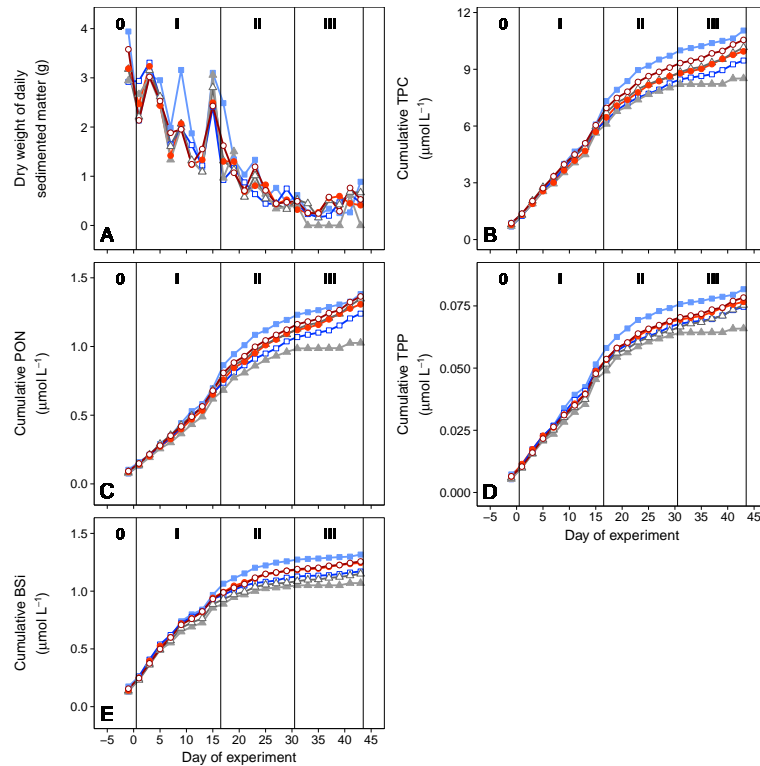


Figure 18. Temporal dynamics in (a) collected sediment trap material mass and cumulative (b) total particulate carbon, (c) particulate organic nitrogen, (d) total particulate phosphorus, (e) particulate biogenic silica. Concentrations in (b–e) were calculated based on individual mesocosm volumes determined at the end of the study. Colours and symbols for different treatments are described in Table 2.